Multiple-Input Multiple-Output OFDM With Index Modulation: Low-Complexity Detector Design

Beixiong Zheng, Miaowen Wen, *Member, IEEE*, Ertugrul Basar, *Senior Member, IEEE*, and Fangjiong Chen, *Member, IEEE*

***Abstract*—Multiple-input multiple-output orthogonal frequency division multiplexing with index modulation (MIMO-OFDM-IM), which provides a flexible trade-off between spectral efficiency and error performance, is recently proposed as a promising transmission technique for energy-efficient 5G wireless communications systems. However, due to the dependence of subcarrier symbols within each subblock and the strong interchannel interference, it is challenging to detect the transmitted data effectively while imposing low computational burden to the receiver. In this paper, we propose two types of low-complexity detectors based on the sequential Monte Carlo (SMC) theory for the detection of MIMO-OFDM-IM signals. The first detector draws samples independently at the subblock level, while the second detector draws samples at the subcarrier level with further reduced complexity. To meet the constraint of the subcarrier combinations within each subblock, the second detector is further coupled with a carefully designed legality examination method. Attributed to the effectiveness of legality examination and deterministic SMC sampling, both proposed detectors achieve near-optimal error performance for the MIMO-OFDM-IM system.**

***Index Terms*—OFDM with index modulation (OFDM-IM), spatial modulation (SM), MIMO systems, sequential Monte Carlo (SMC), maximum-likelihood (ML) detection.**

I. Introduction

With the increasing demand for higher spectral efficiency and reliability in the next generation wireless communications, multiple-input multiple-output (MIMO) systems have been receiving great attention for their ability in improving the transmission rate and error performance [1]–[3]. Recently, a novel MIMO scheme called spatial modulation (SM) has emerged as an appealing candidate to fulfill the spectral and energy efficiency requirements of the next generation wireless communication systems [4]–[10]. In SM, information bits are conveyed by not only the modulated symbol but also the index of the active transmit antenna. Compared with classical MIMO, SM has a number of advantages, including reduced interchannel interference, relaxed inter-antenna synchronization requirements, and reduced receiver complexity [6], [7]. Owing to its various advantages, design and analysis of SM transmission in various scenarios, e.g., adaptive SM [11]–[13], generalized SM [14]–[16], and energy evaluation of SM [17]–[20], are extensively investigated. Specially, for practical multipath fading channels, single-carrier aided SM [21]–[23] is conceived as an appealing technique to eliminate inter-antenna interference and achieve high energy efficiency with only one active antenna at any time instant. Compared with single-carrier transmission, orthogonal frequency division multiplexing (OFDM) is usually more favored for multipath fading channels as it facilitates low-complexity receiver design by converting the multipath fading channel into several parallel flat fading channels in the expense of an increased peak-to-average-power ratio (PAPR) at the transmitter.

By replacing the antenna indices in the MIMO system with the subcarrier indices of the OFDM signal, the concept of SM has been successfully transplanted to OFDM systems [24]–[27]. As the representative frequency-domain extension of SM, OFDM with index modulation (OFDM-IM), which activates a subset of subcarriers to carry the modulated symbols simultaneously, is proposed in [26]. In OFDM-IM, the information is embedded in both subcarrier indices and M-ary constellation domains. Compared with classical OFDM, OFDM-IM provides a more flexible trade-off between the spectral efficiency and the error performance [28], and has the potential to achieve much better bit error rate (BER) performance for low-to-mid spectral efficiencies [26].

Owing to its interesting properties and superior BER performance, OFDM-IM has attracted considerable research interest over the past few years [28]–[42]. A subcarrier-level interleaving method is proposed for OFDM-IM to attain coding gains from uncorrelated subcarriers [29], [30]. In [31], OFDM-IM coupled with the coordinate interleaving principle is proposed to explore potential diversity gains of OFDM-IM. By extending the index modulation to include both the in-phase and quadrature dimensions, a generalization of OFDM-IM is proposed in [32]. Following [32], a low-complexity maximum-likelihood (ML)

Manuscript received August 7, 2016; revised December 28, 2016; accepted January 28, 2017. Date of publication February 23, 2017; date of current version March 24, 2017. The associate editor coordinating the review of this manuscript and approving it for publication was Dr. Yue Rong. This work was supported in part by the National Natural Science Foundation of China under Grant 61431005, Grant 61501190, Grant 61671211, in part by the Natural Science Foundation of Guangdong Province under Grant 2016A030311024, in part by the open research fund of National Mobile Communications Research Laboratory, Southeast University under Grant 2017D08, and in part by the China Scholarship Council. *(Corresponding author: Miaowen Wen.)*

B. Zheng and F. Chen are with the School of Electronic and Information Engineering, South China University of Technology, Guangzhou 510641, China (e-mail: zheng.bx@mail.scut.edu.cn; eefjchen@scut.edu.cn).

M. Wen is with the School of Electronic and Information Engineering, South China University of Technology, Guangzhou 510641, China, and also with National Mobile Communications Research Laboratory, Southeast University, Nanjing 210096, China (e-mail: eemwwen@scut.edu.cn).

E. Basar is with the Istanbul Technical University, Faculty of Electrical and Electronics Engineering, Istanbul 34469, Turkey (e-mail: basarer@itu.edu.tr).

Color versions of one or more of the figures in this paper are available online at http://ieeexplore.ieee.org.

Digital Object Identifier 10.1109/TSP.2017.2673803

detector is developed in [28]. By introducing the index modulation in both space and frequency domains, a generalization of space-frequency index modulation is proposed to convey information via antenna index, subcarrier index, and M-ary modulation bits [33]. To reduce the intercarrier interference caused by Doppler shift and/or transceiver imperfection, OFDM-IM merged with intercarrier interference self-cancellation is proposed in [34]. In [35], a hybrid OFDM-IM technique is proposed to enhance the spectral efficiency and deal with the severe intercarrier interference problem encountered in underwater acoustic communications. In [36] and [37], the optimal number of active subcarriers selection problem is investigated. In recent times, the performance of OFDM-IM is analyzed in terms of ergodic achievable rate [38] and average mutual information [39].

Due to the advantages of OFDM and MIMO transmission techniques, the combination of them has been regarded as a promising solution for enhancing the data rates of next generation wireless communications systems. More recently, by combining OFDM-IM with MIMO transmission techniques, a novel MIMO-OFDM with index modulation (MIMO-OFDM-IM) scheme is presented in [40], which exhibits the potential to surpass the classical MIMO-OFDM. Specifically, by deactivating a subset of subcarriers, MIMO-OFDM-IM has the potential to achieve much better BER performance than classical MIMO-OFDM, resulting in higher energy efficiency for practical systems. Then, the error performance of the MIMO-OFDM-IM scheme is investigated theoretically for different types of detectors in [41] and its adaptation to visible light communication systems is presented in [42]. In this scheme, since each transmit antenna transmits an independent OFDM-IM block, its spectral efficiency can reach N_t times that of OFDM-IM, where N_t denotes the number of transmit antennas. Inheriting from OFDM-IM, MIMO-OFDM-IM is also able to provide an interesting trade-off between the spectral efficiency and the error performance by adjusting the number of active subcarriers in each OFDM-IM subblock. However, due to the dependence of the subcarrier symbols within each OFDM-IM subblock and the strong inter-channel interference (ICI) between the transmit antennas of the MIMO-OFDM-IM system, it becomes much more challenging to detect the active subcarrier indices and modulated symbols. Although the ML detector is able to achieve optimal performance, it necessitates an exhaustive search with prohibitive computational complexity, which makes itself impractical for MIMO-OFDM-IM. To reduce the detection complexity, several low complexity detectors, e.g., simple minimum mean square error (MMSE) detector, log-likelihood ratio (LLR) based MMSE detector, and ordered successive interference cancellation (OSIC) based MMSE detector are proposed for the detection of MIMO-OFDM-IM [40], [41]. However, those existing low complexity detectors suffer from a significant error performance loss compared to the ML detector. Therefore, the design of low-complexity detection algorithms for MIMO-OFDM-IM with near-optimal error performance remains an open as well as challenging research problem.

In this paper, in order to achieve near-optimal error performance while maintaining low computational complexity, two types of detection algorithms based on the sequential Monte Carlo (SMC) theory are proposed for MIMO-OFDM-IM. By regarding each OFDM-IM subblock as a super modulated symbol drawn from a large finite set, the first type of detector draws samples independently at the subblock level. Although it is capable of achieving near-optimal performance with substantially reduced complexity, its decoding complexity can be still unsatisfactory when the size of the OFDM-IM subblock grows much larger. To further reduce the complexity, the second type of detector is proposed to draw samples subcarrier-wise from the modified constellation with a much smaller size. To meet the constraint on the legal active subcarrier combinations within each OFDM-IM subblock, the second type of detector is coupled with a carefully designed examination method to avoid illegal samples. Thanks to the effectiveness of the deterministic SMC sampling and legality examination, it only suffers from a marginal error performance loss. Finally, computer simulation and numerical results in terms of BER and number of complex multiplications (NCM) corroborate the superiority of both proposed detection methods.

The rest of this paper is organized as follows. Section II introduces the system model of MIMO-OFDM-IM. Section III gives a brief introduction of deterministic SMC and a sequential structure of MIMO-OFDM-IM. The deterministic SMC aided detection methods are developed in Section IV. The computational complexity of different detection methods is analyzed and compared in Section V. Section VI provides the computer simulation and numerical results. Finally, conclusions are given in Section VII.

Notation: Upper and lower case boldface letters denote matrices and column vectors, respectively. $(\cdot)^{\mathrm{T}}$, $(\cdot)^{\mathrm{H}}$, and $(\cdot)^{-1}$ stand for transpose, Hermitian transpose, and matrix inversion operations, respectively. $(\cdot)^{(b)}$ denotes the b-th particle drawn by the SMC sampling, its associated importance weight, or its prediction distribution. $(\cdot)_{[i]}$ denotes the hypothesis drawn with the sample being the i-th element of a finite set, its associated importance weight, or its prediction distribution. $\{x_n\}_{n=1}^{N}$ denotes a N-size set, whose elements are $x_1, \ldots, x_N$. $\mathrm{diag}\{\mathbf{x}\}$ returns a diagonal matrix whose diagonal elements are included in $\mathbf{x}$. $|\cdot|$ denotes the absolute value if applied to a complex number or the cardinality if applied to a set. The probability density function (PDF) and the probability mass function (PMF) are denoted by $p(\cdot)$ and $P(\cdot)$, respectively. $\psi(\cdot)$ represents the trial distribution chosen for the SMC sampling. $E\{\cdot\}$ stands for expectation and $\lfloor\cdot\rfloor$ denotes the floor function. The order of detection complexity with respect to the constellation size is denoted by $\mathcal{O}(\cdot)$. $\|\cdot\|_p$ denotes the ℓ_p-norm and $\emptyset$ represents the empty set. $\mathrm{count}(\cdot)$ returns the number of non-zero elements in a set or a vector. $\binom{N}{K}$ denotes the binomial coefficient, which is defined to be zero if $N < K$.

II. Overview of MIMO-OFDM-IM

In this paper, we consider a MIMO-OFDM-IM system equipped with N_t transmit and N_r receive antennas [40], [41]. The block diagram of the MIMO-OFDM-IM transmitter is depicted in Fig. 1. Each MIMO-OFDM-IM frame is comprised of a total number of mN_t incoming data bits. These bits are divided into N_t groups for N_t transmit antennas, each of which

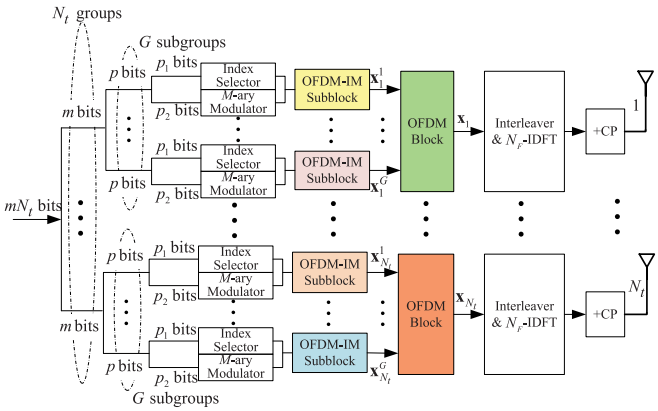

Fig. 1. Block diagram of MIMO-OFDM-IM transmitter.

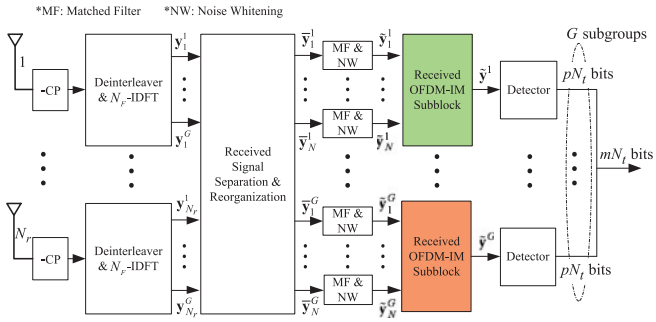

Fig. 2. Block diagram of MIMO-OFDM-IM receiver.

contains m bits for the generation of an OFDM-IM block to be transmitted from a transmit antenna. These m bits are further divided into G subgroups, each of which consists of p bits, i.e., $m = Gp$. Assuming N_F available subcarriers of each block, each subgroup is then used to generate an OFDM-IM subblock consisting of $N = N_F/G$ subcarriers.

Unlike classical OFDM, which maps all data bits to the constellation points for all subcarriers, OFDM-IM separates p bits of each subblock into two parts for different purposes: the first part with $p_1 = \lfloor \log_2 \binom{N}{K} \rfloor$ bits is used to select K active subcarriers, while the remaining $N - K$ subcarriers are set to be idle;[1] the second part with $p_2 = K \log_2 M$ bits is mapped into K modulated symbols for the K active subcarriers via M-ary modulation. The mapping between the p_1 bits and the subcarrier combination patterns can be implemented by using a look-up table or the combinatorial method [26]. Consider the g-th ($1 \le g \le G$) OFDM-IM subblock at the t-th ($1 \le t \le N_t$) transmit antenna. Accordingly, the output of the first part should be the indices of K active subcarriers, which are given by the following set:

$$J_t^g = \{j_t^g(1), \ldots, j_t^g(K)\} \tag{1}$$

where $j_t^g(k) \in \{1, \ldots, N\}$ for $k = 1, \ldots, K$, and the elements of J_t^g are sorted in an ascending order, i.e., $j_t^g(1) < j_t^g(2) < \cdots < j_t^g(K)$. The output of the second part should be K modulated symbols $\{s_t^g(n)\}_{n \in J_t^g}$, where $s_t^g(n)$ is drawn from a complex alphabet $\tilde{\mathcal{S}}$ with $|\tilde{\mathcal{S}}| = M$ and we assume that $E\{|s_t^g(n)|^2\} = 1$ for the normalization of signal constellation. Therefore, the g-th OFDM-IM subblock element at the t-th transmit antenna can be expressed as $\mathbf{x}_t^g = [x_t^g(1)\ x_t^g(2)\ \cdots\ x_t^g(N)]^{\mathrm{T}}$, where

$$x_t^g(n) = \begin{cases} s_t^g(n), & n \in J_t^g \\ 0, & \text{otherwise} \end{cases}. \tag{2}$$

From above, it is clear that each subblock of the MIMO-OFDM-IM contains a fixed number of active subcarriers, whose positions carry information through the subcarrier indices.

[1]Note that to modulate an integer number of bits, only $N_C = 2^{p_1}$ subcarrier combination patterns are permitted and the remaining $\binom{N}{K} - N_C$ patterns are considered to be illegal.

After generating all OFDM-IM subblocks, each OFDM-IM block is created by concatenating G OFDM-IM subblocks in each branch of the transmitter, which is denoted by $\mathbf{x}_t = [(\mathbf{x}_t^1)^{\mathrm{T}}\ (\mathbf{x}_t^2)^{\mathrm{T}}\ \cdots\ (\mathbf{x}_t^G)^{\mathrm{T}}]^{\mathrm{T}} \triangleq [x_t(1)\ x_t(2)\ \cdots\ x_t(N_F)]^{\mathrm{T}}$, where $1 \le t \le N_t$. To fully benefit from the frequency-selective fading, a $G \times N$ block interleaver (a.k.a. OFDM-IM with interleaved grouping in [29], [38]) is employed in each branch of the transmitter. Before transmission, each OFDM-IM block is first transformed into the time-domain signal block by employing an N_F-point inverse discrete Fourier transform (IDFT), and then appended with a CP of length N_{cp}, which is longer than the maximum delay spread of the channel. The spectral efficiency of MIMO-OFDM-IM, measured in terms of bit/s/Hz, is thus given by

$$\eta = \frac{mN_t}{N_F + N_{cp}} = N_t \frac{\lfloor \log_2 \binom{N}{K} \rfloor}{N + N_{cp}/G} + N_t \frac{K \log_2 M}{N + N_{cp}/G}. \tag{3}$$

As shown in Fig. 2, after passing through the frequency-selective MIMO channel, the CP is removed and an N_F-point discrete Fourier transform (DFT) followed by a $G \times N$ block deinterleaver is employed at each receive antenna to obtain the received block in the frequency domain. Specifically, for the r-th ($1 \le r \le N_r$) receive antenna, the g-th ($1 \le g \le G$) received subblock after block deinterleaving can be expressed as

$$\mathbf{y}_r^g = \sqrt{\frac{\rho}{N_t}} \sqrt{\frac{N}{K}} \sum_{t=1}^{N_t} \mathrm{diag}\left\{\mathbf{h}_{r,t}^g\right\} \mathbf{x}_t^g + \mathbf{w}_r^g \tag{4}$$

where $\mathbf{y}_r^g \triangleq [y_r^g(1)\ y_r^g(2)\ \cdots\ y_r^g(N)]^{\mathrm{T}}$, ρ is signal-to-noise ratio (SNR) per receive antenna, $\mathbf{h}_{r,t}^g$ denotes the corresponding channel vector of dimensions $N \times 1$ which contains the channel frequency responses (CFRs) for the g-th OFDM-IM subblock, and $\mathbf{w}_r^g$ is the $N \times 1$ vector comprised of zero-mean independent additive white Gaussian noise (AWGN) samples with unit variance. Here the factor $\sqrt{\frac{N}{K}}$ is applied at the transmitter to balance the total transmit power, which is referred to as power reallocation in [24] and [38]. Furthermore, for the n-th ($1 \le n \le N$) subcarrier of the g-th ($1 \le g \le G$) OFDM-IM subblock, the signal vector observed at the receiver can be

collected as

$$\underbrace{\begin{bmatrix} y_1^g(n) \\ y_2^g(n) \\ \vdots \\ y_{N_r}^g(n) \end{bmatrix}}_{\bar{\mathbf{y}}_n^g} = \sqrt{\frac{\rho}{N_t}}\sqrt{\frac{N}{K}} \underbrace{\begin{bmatrix} h_{1,1}^g(n) & h_{1,2}^g(n) & \dots & h_{1,N_t}^g(n) \\ h_{2,1}^g(n) & h_{2,2}^g(n) & \dots & h_{2,N_t}^g(n) \\ \vdots & \vdots & \ddots & \vdots \\ h_{N_r,1}^g(n) & h_{N_r,2}^g(n) & \dots & h_{N_r,N_t}^g(n) \end{bmatrix}}_{\bar{\mathbf{H}}_n^g} \times \underbrace{\begin{bmatrix} x_1^g(n) \\ x_2^g(n) \\ \vdots \\ x_{N_t}^g(n) \end{bmatrix}}_{\bar{\mathbf{x}}_n^g} + \underbrace{\begin{bmatrix} w_1^g(n) \\ w_2^g(n) \\ \vdots \\ w_{N_r}^g(n) \end{bmatrix}}_{\bar{\mathbf{w}}_n^g} \tag{5}$$

where $\bar{\mathbf{y}}_n^g$ is the received signal vector, $\bar{\mathbf{H}}_n^g$ is the corresponding channel matrix which contains the CFRs between the transmit and receive antennas at the n-th subcarrier, $\bar{\mathbf{x}}_n^g$ is the data vector which contains the simultaneously transmitted symbols from all transmit antennas at the n-th subcarrier, and $\bar{\mathbf{w}}_n^g$ is an $N_r \times 1$ AWGN vector whose elements have zero mean and unit variance. After applying the matched filter and noise whitening[2] to (5), the output can be written as

$$\begin{aligned} \tilde{\mathbf{y}}_n^g &\triangleq \left(\mathbf{A}_n^g\right)^{-1/2} \left(\bar{\mathbf{H}}_n^g\right)^{\mathrm{H}} \bar{\mathbf{y}}_n^g \\ &= \sqrt{\frac{\rho}{N_t}}\sqrt{\frac{N}{K}} \left(\mathbf{A}_n^g\right)^{1/2} \bar{\mathbf{x}}_n^g + \tilde{\mathbf{w}}_n^g \end{aligned} \tag{6}$$

where $\mathbf{A}_n^g = (\bar{\mathbf{H}}_n^g)^{\mathrm{H}}\bar{\mathbf{H}}_n^g$, and $\tilde{\mathbf{w}}_n^g = (\mathbf{A}_n^g)^{-1/2}(\bar{\mathbf{H}}_n^g)^{\mathrm{H}}\bar{\mathbf{w}}_n^g$ is an $N_t \times 1$ AWGN vector whose elements have zero-mean and unit variance. Let us stack the received signal vectors in (6) for N consecutive subcarriers of the g-th ($1 \le g \le G$) OFDM-IM subblock, which can be expressed as

$$\underbrace{\begin{bmatrix} \tilde{\mathbf{y}}_1^g \\ \tilde{\mathbf{y}}_2^g \\ \vdots \\ \tilde{\mathbf{y}}_N^g \end{bmatrix}}_{\tilde{\mathbf{y}}^g} = \sqrt{\frac{\rho}{N_t}}\sqrt{\frac{N}{K}} \underbrace{\begin{bmatrix} \left(\mathbf{A}_1^g\right)^{1/2} & \mathbf{0} & \dots & \mathbf{0} \\ \mathbf{0} & \left(\mathbf{A}_2^g\right)^{1/2} & \dots & \mathbf{0} \\ \vdots & \vdots & \ddots & \vdots \\ \mathbf{0} & \mathbf{0} & \dots & \left(\mathbf{A}_N^g\right)^{1/2} \end{bmatrix}}_{\tilde{\mathbf{A}}^g} \times \underbrace{\begin{bmatrix} \bar{\mathbf{x}}_1^g \\ \bar{\mathbf{x}}_2^g \\ \vdots \\ \bar{\mathbf{x}}_N^g \end{bmatrix}}_{\tilde{\mathbf{x}}^g} + \underbrace{\begin{bmatrix} \tilde{\mathbf{w}}_1^g \\ \tilde{\mathbf{w}}_2^g \\ \vdots \\ \tilde{\mathbf{w}}_N^g \end{bmatrix}}_{\tilde{\mathbf{w}}_n^g} \tag{7}$$

[2]The matched filter and noise whitening maximize the received SNR without changing the noise whitening characteristics.

where $\tilde{\mathbf{y}}^g$ is the received signal vector after stacking, $\tilde{\mathbf{A}}^g$ is a block diagonal channel matrix whose diagonal elements are $(\mathbf{A}_n^g)^{1/2}$ with $n = 1, \dots, N$ and the off-diagonal elements are zero matrices $\mathbf{0}$ of size $N_t \times N_t$, $\tilde{\mathbf{x}}^g$ is the data vector after stacking all g-th OFDM-IM subblocks, and $\tilde{\mathbf{w}}^g$ is a $N_t N \times 1$ AWGN vector whose elements have zero-mean and unit variance.

By considering a joint detection for all g-th OFDM-IM subblocks from different transmit antennas, the ML detector based on (7) for MIMO-OFDM-IM is given by

$$\hat{\tilde{\mathbf{x}}}^g = \arg\min_{\tilde{\mathbf{x}}^g} \left\| \tilde{\mathbf{y}}^g - \sqrt{\frac{\rho}{N_t}}\sqrt{\frac{N}{K}} \tilde{\mathbf{A}}^g \tilde{\mathbf{x}}^g \right\|^2. \tag{8}$$

Although the ML detector can achieve optimal error performance, its computational complexity increases exponentially with the size of subblock and the number of transmit antennas. From (8), it can be observed that the search complexity per subblock is of order $(N_C M^K)^{N_t}$ for the ML detector, which is costly and even infeasible for the practical implementation of the receiver.

Considering the immense computational complexity required by the ML detector, the MMSE-LLR detector is developed later in [40] and [41] to solve this drawback. In this detector, the MMSE filter is first employed to decouple the superimposed OFDM-IM subblocks at the receiver, and a sophisticated LLR calculator is then applied to determine the indices of the active subcarriers. Although this detector exhibits significantly reduced complexity due to the decoupling of the subblocks, its performance is far inferior to that of the ML detector. Therefore, it is very demanding to design a more effective detector for MIMO-OFDM-IM while maintaining low detection complexity at the receiver. To this end, we propose two novel detectors based on the SMC theory.

III. Introduction to Deterministic SMC and Sequential Structure for MIMO-OFDM-IM

The SMC method, also referred to as particle filter, is a class of the sampling based sequential Bayesian inference methodologies for general dynamic systems, which has been widely applied in wireless communications [43]–[48]. In the following, we will first briefly introduce the concept of the deterministic SMC and then construct the sequential structure for MIMO-OFDM-IM.

A. Basic Concept of Deterministic SMC

In most applications of digital communications, the transmitted signals take values from a finite set and the received signals are the superimposition of transmitted signals corrupted by Gaussian noise. The *a posteriori* distribution can be thus computed by performing an exhaustive search over all possible realizations of the transmitted signal block, whose computational complexity grows exponentially with the size of the transmitted signal block. Instead of the exhaustive search and computation, the objective of the deterministic SMC method is to numerically approximate the *a posteriori* distributions of the states of some Markov processes, given some noisy and partial observations. At each sampling interval, we draw symbol samples from the given finite set to construct new sequential particles, and then update their corresponding importance weights, where an

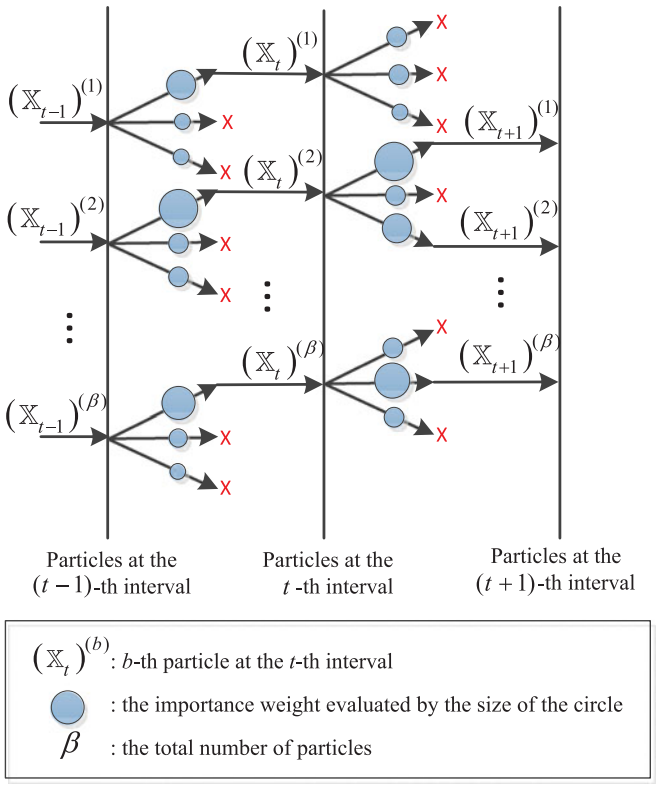

Fig. 3. Illustration of the deterministic SMC.

illustrative example is shown in Fig. 3. Specifically, after calculating the importance weights for all hypotheses generated by the previous particles $\{(\mathbb{X}_{t-1})^{(b)}\}_{b=1}^{\beta}$, we only retain β most promising hypotheses associated with the highest importance weights as the new particles $\{(\mathbb{X}_t)^{(b)}\}_{b=1}^{\beta}$ while discarding other hypotheses immediately at each sampling interval. More detailed descriptions of the deterministic SMC concept will be given in Section IV with the proposed algorithms.

It has been shown that the deterministic SMC-based detectors can achieve near-ML performance with much lower computational cost to the receiver for various communications systems [43]–[48]. Moreover, attributed to its nature of being soft-input and soft-output, SMC based detection can also be efficiently employed in coded communication systems. However, to apply the deterministic SMC theory in a specific system, it is essential to construct the sequential structure based on the observed signals for the sampling procedure, which varies for different communication scenarios.

B. Sequential Structure for MIMO-OFDM-IM

To apply the SMC theory to the detection of MIMO-OFDM-IM, we construct the sequential structure based on the observed signals in the sequel. Inspired by the successive interference cancellation (SIC) method for the MIMO detection [49], we apply the QL decomposition[3] to the matrix $(\mathbf{A}_n^g)^{1/2}$ in (6) as

$$(\mathbf{A}_n^g)^{1/2} = \mathbf{Q}_n^g \mathbf{L}_n^g, \qquad n = 1, \ldots, N,\ g = 1, \ldots, G \tag{9}$$

[3]The QL decomposition can be obtained in analogy with the QR decomposition, which can be derived by using the Gram-Schmidt process starting from the last column of the designated matrix.

where $\mathbf{Q}_n^g$ is a unitary matrix, and $\mathbf{L}_n^g$ is a lower triangular matrix. The lower triangular operation is carried out by the left multiplication of the vector $\tilde{\mathbf{y}}_n^g$ in (6) by $(\mathbf{Q}_n^g)^{\mathrm{H}}$ to obtain $\bar{\mathbf{z}}_n^g = (\mathbf{Q}_n^g)^{\mathrm{H}} \tilde{\mathbf{y}}_n^g$, which can be further written as

$$\underbrace{\begin{bmatrix} z_1^g(n) \\ z_2^g(n) \\ \vdots \\ z_{N_t}^g(n) \end{bmatrix}}_{\bar{\mathbf{z}}_n^g} = \sqrt{\frac{\rho}{N_t}} \sqrt{\frac{N}{K}} \underbrace{\begin{bmatrix} l_{1,1}^g(n) & & & \\ l_{2,1}^g(n) & l_{2,2}^g(n) & & \\ \vdots & \vdots & \ddots & \\ l_{N_t,1}^g(n) & l_{N_t,2}^g(n) & \ldots & l_{N_t,N_t}^g(n) \end{bmatrix}}_{\mathbf{L}_n^g} \times \underbrace{\begin{bmatrix} x_1^g(n) \\ x_2^g(n) \\ \vdots \\ x_{N_t}^g(n) \end{bmatrix}}_{\bar{\mathbf{x}}_n^g} + \underbrace{\begin{bmatrix} v_1^g(n) \\ v_2^g(n) \\ \vdots \\ v_{N_t}^g(n) \end{bmatrix}}_{\bar{\mathbf{v}}_n^g} \tag{10}$$

where $\bar{\mathbf{v}}_n^g = (\mathbf{Q}_n^g)^{\mathrm{H}} \tilde{\mathbf{w}}_n^g$ is still an $N_t \times 1$ zero-mean AWGN vector with unit variance elements as the matrix $\mathbf{Q}_n^g$ is unitary. Based on the structure in (10), the SIC may be applied to detect the data vector $\bar{\mathbf{x}}_n^g$ in a sequential manner, i.e., the interference due to the previously decoded symbols is subtracted from the currently observed sample before decoding the next symbol. However, one should keep in mind that unlike the classical MIMO-OFDM in which the symbols carried on the different subcarriers are independently generated, the symbols carried on different subcarriers within each OFDM-IM subblock are binded together in the MIMO-OFDM-IM due to the index modulation. Therefore, to be suited to MIMO-OFDM-IM, the SIC method for MIMO-OFDM-IM has to be performed in a subblock-by-subblock manner, resulting in a search complexity as high as of order $N_t N_C M^K$. Moreover, the SIC method may suffer from the problem of error propagation, which also limits its error performance. In this paper, we will not employ the SIC method but instead exploit the aforementioned sequential structure for the low-complexity detector design of MIMO-OFDM-IM.

IV. Low-Complexity Detectors for MIMO-OFDM-IM

In this section, we will develop two types of SMC-based detectors by using the structure of (10) as the kernel for MIMO-OFDM-IM. As will be shown by computer simulations, the new algorithms can avoid error propagation successfully and provide near-optimal error performance for MIMO-OFDM-IM.

A. Deterministic SMC Aided Subblock-Wise Detection

After the lower triangular operation, the sequential structure in (10) can be exploited by applying the SMC method to draw samples starting from the first transmit antenna and ending to the

last one. Indeed, if we simply regard each OFDM-IM subblock $\mathbf{x}_t^g$ as a super modulated symbol drawn from a large finite set, we have the *a posteriori* distribution of $\{\mathbf{x}_t^g\}_{t=1}^{N_t}$ conditioned on $\{\mathbf{z}_t^g\}_{t=1}^{N_t}$ as

$$P\left(\{\mathbf{x}_t^g\}_{t=1}^{N_t}\,\middle|\,\{\mathbf{z}_t^g\}_{t=1}^{N_t}\right) \propto \prod_{t=1}^{N_t} p\left(\mathbf{z}_t^g\middle|\mathbb{X}_t^g\right) P\left(\mathbf{x}_t^g\right) \tag{11}$$

where $\mathbf{z}_t^g \triangleq [z_t^g(1)\ z_t^g(2)\ \cdots\ z_t^g(N)]^{\mathrm{T}}$ denotes the observed subblock in the t-th ($1 \le t \le N_t$) branch of the receiver after the lower triangular operation in (10), and $\mathbb{X}_t^g \triangleq \{\mathbf{x}_{t'}^g\}_{t'=1}^{t}$. Based on (11), we construct the sequence of probability distributions $\{P(\mathbb{X}_t^g|\mathbb{Z}_t^g)\}_{t=1}^{N_t}$, which can be expressed as

$$P\left(\mathbb{X}_t^g\middle|\mathbb{Z}_t^g\right) \propto \prod_{t'=1}^{t} p\left(\mathbf{z}_{t'}^g\middle|\mathbb{X}_{t'}^g\right) P\left(\mathbf{x}_{t'}^g\right), \quad t = 1, \ldots, N_t \tag{12}$$

where $\mathbb{Z}_t^g \triangleq \{\mathbf{z}_{t'}^g\}_{t'=1}^{t}$. From the perspective of the probability theory, our aim is to estimate the *a posteriori* probability of each OFDM-IM subblock

$$P\left(\mathbf{x}_t^g = \mathbf{\Phi}_i\middle|\,\{\mathbf{z}_t^g\}_{t=1}^{N_t}\right),\ \mathbf{\Phi}_i \in \tilde{\mathbf{\Phi}},\ t = 1, \ldots, N_t \tag{13}$$

based on the observed subblocks $\{\mathbf{z}_t^g\}_{t=1}^{N_t}$, where $\tilde{\mathbf{\Phi}} \triangleq \{\mathbf{\Phi}_i\}_{i=1}^{N_C M^K}$ with $|\tilde{\mathbf{\Phi}}| = N_C M^K$ denotes the set including all possible realizations of the OFDM-IM subblock. Instead of the direct computation of (13), which is too computationally expensive, we seek to numerically approximate (13) by using the deterministic SMC theory to substantially reduce the complexity at the receiver.

Let $(\mathbb{X}_t^g)^{(b)}$ with $b = 1, \ldots, \beta$ be the particles drawn by the SMC method at the t-th sampling interval on the basis of subblock, where β denotes the total number of particles. To implement the SMC method, we first generate a set of incomplete particles for the OFDM-IM subblocks, and then update the corresponding importance weights for those particles with respect to the distribution of (11) until the subblock at the last antenna is reached. Moreover, to update the importance weights, it is crucial to design the trial distribution which minimizes the variance of the importance weights conditioned upon the previous particles and the observed signals [50]. Under the criterion of minimum conditional variance of the importance weights, we simply choose the trial distribution as

$$\psi\left(\mathbf{x}_t^g\middle|\mathbb{Z}_t^g, \left(\mathbb{X}_{t-1}^g\right)^{(b)}\right) \propto P\left(\mathbf{x}_t^g\middle|\mathbb{Z}_t^g, \left(\mathbb{X}_{t-1}^g\right)^{(b)}\right) \tag{14}$$

for $t = 1, \ldots, N_t$.

Proposition 1: With the trial distribution given in (14), the importance weight for the SMC can be updated according to

$$\left(\varpi_t^g\right)^{(b)} \propto \left(\varpi_{t-1}^g\right)^{(b)} \cdot p\left(\mathbf{z}_t^g\middle|\left(\mathbb{X}_{t-1}^g\right)^{(b)}\right) \tag{15}$$

where $p(\mathbf{z}_t^g|(\mathbb{X}_{t-1}^g)^{(b)})$ can be regarded as the prediction distribution of the currently observed subblock $\mathbf{z}_t^g$ under the condition of the previous particle $(\mathbb{X}_{t-1}^g)^{(b)}$.

Proof: See Appendix A.

In the MIMO-OFDM-IM system, each OFDM-IM subblock has a finite number of realizations, i.e., $N_C M^K$. For this reason, the deterministic SMC sampling can be applied by first enumerating all possible subblock realizations at each sampling interval and then calculating their associated prediction distributions exactly based on the previous particles paired with the specific subblock sample. In other words, with the given particle $(\mathbb{X}_{t-1}^g)^{(b)}$, we calculate each prediction distribution

$$\left(\gamma_t^g\right)_{[i]}^{(b)} \triangleq p\left(\mathbf{z}_t^g\middle|\mathbf{x}_t^g = \mathbf{\Phi}_i, \left(\mathbb{X}_{t-1}^g\right)^{(b)}\right) \tag{16}$$

for $\mathbf{\Phi}_i \in \tilde{\mathbf{\Phi}}$ to get a more precise result. If the specific subblock sample $\mathbf{x}_t^g = \mathbf{\Phi}_i$ is assumed in the prediction distribution, the update for the importance weight in (15) can be revised as

$$\left(\varpi_t^g\right)_{[i]}^{(b)} \propto \left(\varpi_{t-1}^g\right)^{(b)} \cdot \left(\gamma_t^g\right)_{[i]}^{(b)} \cdot P\left(\mathbf{x}_t^g = \mathbf{\Phi}_i\right) \tag{17}$$

$$\propto \left(\varpi_{t-1}^g\right)^{(b)} \cdot \left(\gamma_t^g\right)_{[i]}^{(b)} \tag{18}$$

where $i = 1, \ldots, N_C M^K$, and (18) holds due to the equal probability assumption for all subblock realizations. Since the noise vector $\bar{\mathbf{v}}_n^g = (\mathbf{Q}_n^g)^{\mathrm{H}} \tilde{\mathbf{w}}_n^g$ in (10) is white Gaussian, the prediction distribution $(\gamma_t^g)_{[i]}^{(b)}$ can be expressed as

$$\left(\gamma_t^g\right)_{[i]}^{(b)} = \frac{1}{\pi^N} \exp\left\{-\left\|\mathbf{z}_t^g - \left(\mathbf{u}_t^g\right)_{[i]}^{(b)}\right\|^2\right\} \tag{19}$$

where $(\mathbf{u}_t^g)_{[i]}^{(b)} \triangleq [(u_t^g(1))_{[i]}^{(b)}\ (u_t^g(2))_{[i]}^{(b)}\ \cdots\ (u_t^g(N))_{[i]}^{(b)}]^{\mathrm{T}}$ denotes the mean vector of $\mathbf{z}_t^g$, whose n-th ($1 \le n \le N$) element is given by

$$\begin{aligned}\left(u_t^g(n)\right)_{[i]}^{(b)} = &\sqrt{\frac{\rho}{N_t}}\sqrt{\frac{N}{K}}\sum_{t'=1}^{t-1} l_{t,t'}^g(n)\left(x_{t'}^g(n)\right)^{(b)} \\ &+ \sqrt{\frac{\rho}{N_t}}\sqrt{\frac{N}{K}} l_{t,t}^g(n)\Phi_i(n)\end{aligned} \tag{20}$$

with $\Phi_i(n)$ being the n-th element of the sample vector $\mathbf{\Phi}_i$.

1) Initialization and Summary of Subblock-wise Algorithm: By assuming the SMC process starts at the Γ-th transmit antenna, we compute the *a posteriori* distributions $P(\mathbb{X}_\Gamma^g|\mathbb{Z}_\Gamma^g)$ exactly by enumerating all possible realizations of $\mathbb{X}_\Gamma^g$, where the total number of possible realizations is $|\tilde{\mathbf{\Phi}}|^\Gamma$ and $\Gamma < N_t$.[4] According to the deterministic SMC and (10), the *a posteriori* probabilities $P((\mathbb{X}_\Gamma^g)^{(b)}|\mathbb{Z}_\Gamma^g)$ can be expressed as

$$P\left(\left(\mathbb{X}_\Gamma^g\right)^{(b)}\middle|\mathbb{Z}_\Gamma^g\right) \propto \prod_{t=1}^{\Gamma}\left(\gamma_t^g\right)_{[i]}^{(b)}. \tag{21}$$

where $b = 1, \ldots, B_\Gamma$, $B_\Gamma = |\tilde{\mathbf{\Phi}}|^\Gamma$, and $\{(\mathbb{X}_\Gamma^g)^{(b)}\}_{b=1}^{B_\Gamma}$ contains all possible realizations of $\mathbb{X}_\Gamma^g$. Then we retain the β particles $\{(\mathbb{X}_\Gamma^g)^{(b)}\}_{b=1}^{\beta}$ with the highest *a posteriori* probabilities as the initial importance weights $\{(\varpi_\Gamma^g)^{(b)}\}_{b=1}^{\beta}$, where $\beta \le B_\Gamma$.

After the initialization, the importance weights are updated according to (18). At each sampling interval on the basis of subblock, current β particles with the highest importance weights are selected as the survivors over $\beta|\tilde{\mathbf{\Phi}}|$ possible hypotheses departed from the previous particles. When the recursion reaches

[4] If $\Gamma \ge N_t$, we can compute $P(\mathbb{X}_{N_t}^g|\mathbb{Z}_{N_t}^g)$ exactly based on the deterministic SMC; however, it is too computationally expensive.

Algorithm 1: Deterministic SMC Aided Subblock-wise Detection.

1: Perform the lower triangular operation to obtain (10);
2: Enumerate all possible realizations of $\mathbb{X}_\Gamma^g$ with their *a posteriori* probabilities given in (21), and retain the β initial particles $\{(\mathbb{X}_\Gamma^g)^{(b)}\}_{b=1}^{\beta}$ with the highest *a posteriori* probabilities as the initial importance weights $\left\{(\varpi_\Gamma^g)^{(b)}\right\}_{b=1}^{\beta}$;
3: **for** $t = \Gamma+1$ to N_t **do**
4: Update the importance weights according to (18), $b = 1, \ldots, \beta$;
5: Pick up and retain β particles with the highest importance weights among the $\beta|\tilde{\mathbf{\Phi}}|$ hypotheses with weights set $\left\{(\varpi_t^g)_{[i]}^{(b)}\right\}$, $b = 1, \ldots, \beta$, $i = 1, \ldots, N_C M^K$;
6: **end for**
7: Compute the *a posteriori* probability for each subblock via (22), and the estimate of each subblock is given by $\widehat{\mathbf{x}}_t^g = \arg\max_{\mathbf{\Phi}_i \in \tilde{\mathbf{\Phi}}} P(\mathbf{x}_t^g = \mathbf{\Phi}_i \big| \{\mathbf{z}_t^g\}_{t=1}^{N_t})$, $t = 1, \ldots, N_t$.

the last sampling interval, i.e., $t = N_t$, β particles and the corresponding importance weights are then used to estimate the *a posteriori* probability for each subblock in (13), given by

$$P\left(\mathbf{x}_t^g = \mathbf{\Phi}_i \Big| \{\mathbf{z}_t^g\}_{t=1}^{N_t}\right) \cong \frac{1}{\widetilde{\varpi}_{N_t}^g} \sum_{b=1}^{\beta} \mathbb{I}\left((\mathbf{x}_t^g)^{(b)}; \mathbf{\Phi}_i\right) \left(\varpi_{N_t}^g\right)^{(b)} \tag{22}$$

where $\mathbf{\Phi}_i \in \tilde{\mathbf{\Phi}}$, $\widetilde{\varpi}_{N_t}^g = \sum_{b=1}^{\beta} (\varpi_{N_t}^g)^{(b)}$, and $\mathbb{I}(;)$ denotes the indicator function [46].

Notably, the importance weights obtained at the last sampling interval is applied to compute the *a posteriori* subblock probabilities, for those weights provide better estimations [51] and we detect the corresponding subblocks at the last step. Moreover, the *a posteriori* probability estimated in (22) can be readily applied to the detection with soft output, which is compatible with the coded system. Finally, we summarize the deterministic SMC aided subblock-wise detection in Algorithm 1.

B. Deterministic SMC Aided Subcarrier-wise Detection

Although the detector proposed in Section IV-A achieves considerable reduction in computational complexity with respect to the ML detector, its complexity still grows exponentially with the size of subblock. To circumvent this problem, we propose another novel detection algorithm based on the deterministic SMC in this subsection, which draws samples at the subcarrier level. To prevent from outputting illegal subblock realization, the subcarrier-wise detector takes into account the constraint of the active subcarrier combinations within each subblock when drawing samples. By exploiting the sequential structure in (10), the subcarrier-wise SMC method detects the information starting from the first transmit antenna and ending to the last transmit antenna and draws samples subcarrier-wise from the first subcarrier to the last subcarrier within the g-th subblock at each transmit antenna.

Considering the dependence of the subcarrier symbols within each subblock, the distribution of (11) can be rewritten at the subcarrier level as

$$P\left(\{\mathbf{x}_t^g\}_{t=1}^{N_t} \Big| \{\mathbf{z}_t^g\}_{t=1}^{N_t}\right) \propto \prod_{t=1}^{N_t}\prod_{n=1}^{N} p\left(z_t^g(n) \Big| \widetilde{\mathbb{X}}_{t,n}^g\right) P\left(x_t^g(n) \Big| \mathbb{x}_{t,n-1}^g\right) \tag{23}$$

where $\widetilde{\mathbb{X}}_{t,n}^g \triangleq \{\mathbb{X}_{t-1}^g, \mathbb{x}_{t,n}^g\}$, $\mathbb{x}_{t,n}^g \triangleq \{x_t^g(n')\}_{n'=1}^{n}$, and $\mathbb{X}_0^g = \mathbb{x}_{t,0}^g = \emptyset$ is defined. Similarly, based on (23), the sequential distributions can be constructed as

$$P\left(\widetilde{\mathbb{X}}_{t,n}^g \Big| \widetilde{\mathbb{Z}}_{t,n}^g\right) \propto \prod_{t'=1}^{t}\prod_{n'=1}^{n} p\left(z_{t'}^g(n') \Big| \widetilde{\mathbb{X}}_{t',n'}^g\right) P\left(x_{t'}^g(n') \Big| \mathbb{x}_{t',n'-1}^g\right) \tag{24}$$

$$\propto P\left(\mathbb{X}_{t-1}^g \Big| \mathbb{Z}_{t-1}^g\right) \prod_{n'=1}^{n} p\left(z_t^g(n') \Big| \widetilde{\mathbb{X}}_{t,n'}^g\right) P\left(x_t^g(n') \Big| \mathbb{x}_{t,n'-1}^g\right) \tag{25}$$

where $t = 1, \ldots, N_t$, $n = 1, \ldots, N$, $\widetilde{\mathbb{Z}}_{t,n}^g \triangleq \{\mathbb{Z}_{t-1}^g, \mathbb{z}_{t,n}^g\}$, $\mathbb{z}_{t,n}^g \triangleq \{z_t^g(n')\}_{n'=1}^{n}$, $\mathbb{Z}_0^g = \mathbb{z}_{t,0}^g = \emptyset$ is defined, and (25) is obtained due to the independence among the subblocks generated from different transmit antennas. Unlike the detector proposed in Section IV-A that estimates the information subblock-wise, the aim of the subcarrier-wise detection is to estimate the *a posteriori* probability at the subcarrier level, which is given by

$$P\left(x_t^g(n) = \mathcal{X}_i \Big| \{\mathbf{z}_t^g\}_{t=1}^{N_t}\right), \ \mathcal{X}_i \in \tilde{\mathcal{X}} \tag{26}$$

where $t = 1, \ldots, N_t$, $n = 1, \ldots, N$, $i = 1, \ldots, M+1$, and $\tilde{\mathcal{X}} \triangleq \{0, \mathcal{S}\}$ with $|\tilde{\mathcal{X}}| = M+1$ denotes the modified constellation. However, due to the dependence of subcarrier symbols within each subblock, it is infeasible to compute (26) directly. Therefore, we resort to the SMC theory by carefully considering this dependent relationship.

Suppose that $(\widetilde{\mathbb{X}}_{t,n}^g)^{(b)}$ with $b = 1, \ldots, \beta$ are the particles drawn by the SMC method at each sampling interval on the basis of subcarrier. Similarly, we can choose the trial distribution as

$$\psi\left(x_t^g(n) \Big| \widetilde{\mathbb{Z}}_{t,n}^g, \left(\widetilde{\mathbb{X}}_{t,n-1}^g\right)^{(b)}\right) \propto P\left(x_t^g(n) \Big| \widetilde{\mathbb{Z}}_{t,n}^g, \left(\widetilde{\mathbb{X}}_{t,n-1}^g\right)^{(b)}\right) \tag{27}$$

for $t = 1, \ldots, N_t$, $n = 1, \ldots, N$.

Proposition 2: With the trial distribution given in (27), the importance weight for the SMC can be updated according to

$$\left(\varpi_{t,n}^g\right)^{(b)} \propto \left(\varpi_{t,n-1}^g\right)^{(b)} \cdot p\left(z_t^g(n) \Big| \left(\widetilde{\mathbb{X}}_{t,n-1}^g\right)^{(b)}\right) \tag{28}$$

where $p(z_t^g(n)\big|(\widetilde{\mathbb{X}}_{t,n-1}^g)^{(b)})$ denotes the prediction distribution of the currently observed signal $z_t^g(n)$ under the condition of the previous particle $(\widetilde{\mathbb{X}}_{t,n-1}^g)^{(b)}$.

Proof: See Appendix B. ■

In MIMO-OFDM-IM, the symbol $x_t^g(n)$ carried on each subcarrier takes values from the modified constellation $\tilde{\mathcal{X}}$ with $|\tilde{\mathcal{X}}| = M+1$. However, those subcarrier symbols within each

subblock are not drawn independently from the finite set $\tilde{\mathcal{X}}$ as they must meet the constraint of the K active subcarrier combinations, which makes the calculation of the exact prediction distribution based on the deterministic SMC method a challenging problem. With a given hypothesis $\{(\widetilde{\mathbb{X}}^g_{t,n-1})^{(b)}, \mathcal{X}_i\}$, we update the importance weight by revising (28) as

$$\left(\varpi^g_{t,n}\right)^{(b)}_{[i]} \propto \left(\varpi^g_{t,n-1}\right)^{(b)} \left(\tilde{\gamma}^g_{t,n}\right)^{(b)}_{[i]} P\left(x^g_t\,(n) = \mathcal{X}_i \middle| \left(\mathbb{X}^g_{t,n-1}\right)^{(b)}\right) \tag{29}$$

where $P(x^g_t(n) = \mathcal{X}_i|(\mathbb{X}^g_{t,n-1})^{(b)})$ indicates the non-independent relationship of subcarrier symbols within each subblock and

$$\left(\tilde{\gamma}^g_{t,n}\right)^{(b)}_{[i]} \triangleq p\left(z^g_t\,(n) \middle| x^g_t\,(n) = \mathcal{X}_i, \left(\widetilde{\mathbb{X}}^g_{t,n-1}\right)^{(b)}\right) \tag{30}$$

denotes the exact prediction distribution. Since the noise vector $\bar{\mathbf{v}}^g_n = (\mathbf{Q}^g_n)^{\mathrm{H}}\tilde{\mathbf{w}}^g_n$ in (10) is white Gaussian, prediction distribution $(\tilde{\gamma}^g_{t,n})^{(b)}_{[i]}$ in (29) can be expressed as

$$\left(\tilde{\gamma}^g_{t,n}\right)^{(b)}_{[i]} = \frac{1}{\pi}\exp\left\{-\left|z^g_t\,(n) - \left(\tilde{u}^g_t\,(n)\right)^{(b)}_{[i]}\right|^2\right\} \tag{31}$$

where $(\tilde{u}^g_t(n))^{(b)}_{[i]}$ denotes the mean of $z^g_t(n)$, which is given by

$$\begin{aligned}\left(\tilde{u}^g_t\,(n)\right)^{(b)}_{[i]} &= \sqrt{\frac{\rho}{N_t}}\sqrt{\frac{N}{K}}\sum_{t'=1}^{t-1} l^g_{t,t'}(n)\left(x^g_{t'}(n)\right)^{(b)} \\ &\quad + \sqrt{\frac{\rho}{N_t}}\sqrt{\frac{N}{K}} l^g_{t,t}(n)\mathcal{X}_i. \end{aligned}\tag{32}$$

For the update of the importance weight in (29), it is essential to determine the conditional probability $P(x^g_t(n) = \mathcal{X}_i\big|(\mathbb{X}^g_{t,n-1})^{(b)})$, as it justifies the dependent relationship of subcarrier symbols within each subblock. In the following, we will give two schemes to calculate the conditional probability $P(x^g_t(n) = \mathcal{X}_i\big|(\mathbb{X}^g_{t,n-1})^{(b)})$.

1) Exhaustive Searching Scheme: According to the Bayes theorem, we can obtain the conditional probability exactly as

$$\begin{aligned} &P\left(x^g_t\,(n) = \mathcal{X}_i \middle| \left(\mathbb{X}^g_{t,n-1}\right)^{(b)}\right) \\ &= \frac{P\left(x^g_t\,(n) = \mathcal{X}_i, \left(\mathbb{X}^g_{t,n-1}\right)^{(b)}\right)}{P\left(\left(\mathbb{X}^g_{t,n-1}\right)^{(b)}\right)} \\ &= \frac{\sum_{\mathbf{\Phi}_i\in\tilde{\mathbf{\Phi}}} P\left(\{\Phi_i(n')\}^n_{n'=1} = \left\{\left(\mathbb{X}^g_{t,n-1}\right)^{(b)}, \mathcal{X}_i\right\}\right)}{\sum_{\mathbf{\Phi}_i\in\tilde{\mathbf{\Phi}}} P\left(\{\Phi_i(n')\}^{n-1}_{n'=1} = \left(\mathbb{X}^g_{t,n-1}\right)^{(b)}\right)} \end{aligned}\tag{33}$$

where $\mathbf{\Phi}_i = [\Phi_i(1)\ \Phi_i(2)\ \cdots\ \Phi_i(N)]^{\mathrm{T}}$. According to (33), if the hypothesis $\{(\mathbb{X}^g_{t,n-1})^{(b)}, \mathcal{X}_i\}$ is illegal, we will have $P(x^g_t(n) = \mathcal{X}_i\big|(\mathbb{X}^g_{t,n-1})^{(b)}) = 0$, such that, the illegal hypotheses can be avoided. However, it is costly to calculate the conditional probability exactly based on (33) as it invokes an exhaustive search over all possible realizations of the OFDM-IM subblock at every sampling interval on the basis of subcarrier.

2) Natural Numbers Mapping Scheme: To strike a trade-off between the complexity cost and the estimation accuracy, we hereafter develop a more efficient method to estimate the conditional probability in (33) and to avoid the propagation of illegal particles. Let us denote the number of non-zero elements in $\mathbb{X}^g_{t,n-1}$ as $\delta^{(b)}_{n-1} = \mathrm{count}((\mathbb{X}^g_{t,n-1})^{(b)})$. Assuming that subcarriers within a subblock are uniformly activated and the modulated symbols are uniformly drawn from an M-ary constellation, we can estimate the conditional probability as

$$\begin{aligned} &P\left(x^g_t\,(n) = \mathcal{X}_i \middle| \left(\mathbb{X}^g_{t,n-1}\right)^{(b)}\right) \\ &\cong \begin{cases} \dfrac{1}{M}\cdot\dfrac{K-\delta^{(b)}_{n-1}}{N-n+1}, & \mathcal{X}_i \in \mathcal{S} \\ \dfrac{N-K+\delta^{(b)}_{n-1}-n+1}{N-n+1}, & \mathcal{X}_i = 0 \end{cases} \end{aligned}\tag{34}$$

where $t = 1,\ldots,N_t,\ n = 1,\ldots,N,$ and $i = 1,\ldots,M+1$. Based on (34), $(\mathbb{X}^g_{t,N})^{(b)}$ with $t = 1,\ldots,N_t$ after the SMC sampling procedure are forced to meet the fixed number constraint of active subcarriers within each subblock, i.e., $\delta^{(b)}_N = K$ for $b = 1,\ldots,\beta$. It is worth pointing out that the calculation of (34) does not involve any specific mapping rule for the subcarrier combination, which is more general and practical. However, when $N_C \neq \binom{N}{K}$, the calculation of (34) will encounter the infiltration of some illegal realizations, i.e., the conditional probabilities of some illegal realizations are not zero. To detect those illegal realizations without using a look-up table, we resort to the combinatorial method in [26] to examine the legality of the realization. The combinatorial method in [26] provides a one-to-one mapping between natural numbers and the combination patterns of K active subcarriers, which is given by

$$\zeta = \binom{j(K)-1}{K} + \cdots + \binom{j(2)-1}{2} + \binom{j(1)-1}{1} \tag{35}$$

where t and g are omitted as (35) is general for all subblocks, and $0 \le \zeta \le \binom{N}{K} - 1$. Based on (35), we can easily examine the legality of the realizations by simply regarding those realizations with $\zeta \ge N_C$ as illegal.

Example 1: Suppose BPSK modulation, $N = 4$ and $K = 2$ and the combinatorial method is applied to determine the indices of the two active subcarriers out of four available subcarriers, as shown in the table in Fig. 4 . The graphical tree is also illustrated in Fig. 4 according to (34). As can be seen, based on (35), we can easily exclude those illegal realizations with $\zeta \ge 4$.

For the calculation based on (34), it can be readily verified that the ratio of the number of the illegal realizations to that of legal ones is $(\binom{N}{K} - N_C)/N_C$, which is typically small. For this reason, we only examine the legality of the particles when they reach the last subcarrier within each subblock, i.e., $n = N$.

Remark 1: As illustrated above, the method based on (34) and (35) does not require any look-up table and is general for different N and K values, which is more efficient and practical than the calculation based on (33). Owing to its simplicity and generality, the calculation based on (34) and (35) will be adopted to estimate the conditional probability $P(x^g_t(n) = \mathcal{X}_i\big|(\mathbb{X}^g_{t,n-1})^{(b)})$ in (29) for our computer simulations in Section VI.

3) Initialization and Summary of Subcarrier-wise Algorithm: We assume that the SMC process starts on the Λ-th

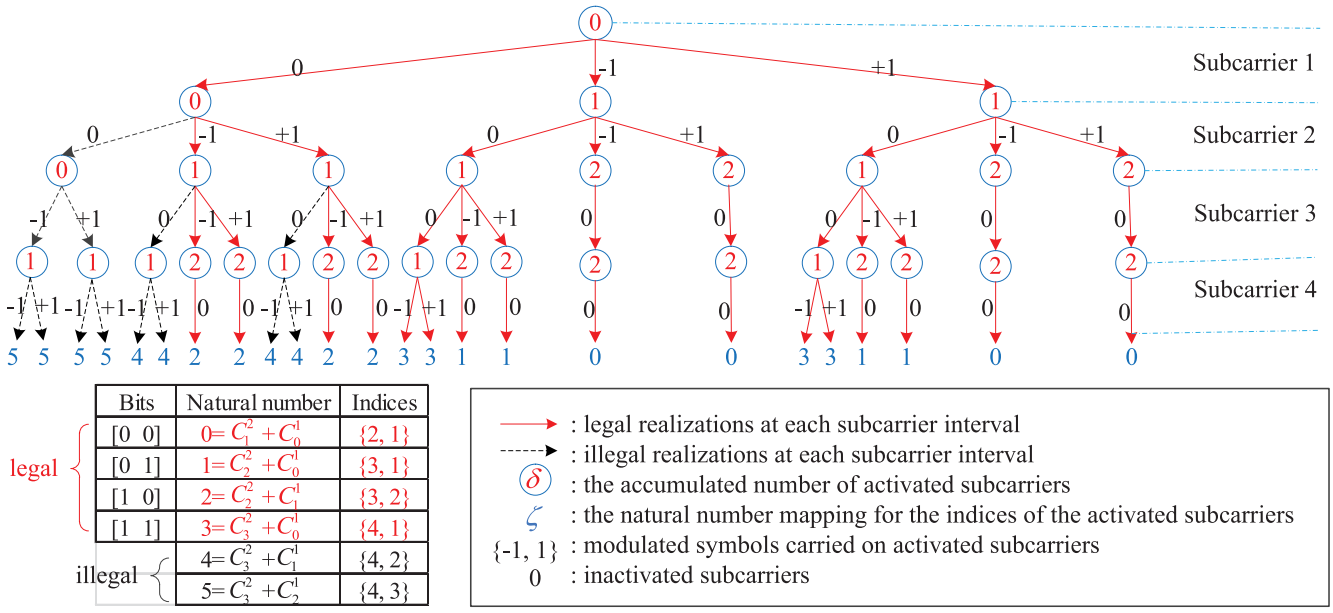

Fig. 4. Illustration of the counter based scheme.

subcarrier of the subblock at the Γ-th transmit antenna and enumerate all legal realizations of $\widetilde{\mathbb{X}}^g_{\Gamma,\Lambda}$, where $\Gamma \le N_t, \Lambda \le N$, and the total number of legal realizations is $\widetilde{B}_{\Gamma,\Lambda} \le |\tilde{\mathbf{\Phi}}|^{\Gamma-1}|\tilde{\mathcal{X}}|^{\Lambda}$.[5] According to the deterministic SMC and (10), we can enumerate all legal realizations of $\widetilde{\mathbb{X}}^g_{\Gamma,\Lambda}$ and compute their *a posteriori* probabilities exactly as

$$P\left(\left(\widetilde{\mathbb{X}}^g_{\Gamma,\Lambda}\right)^{(b)}\middle|\widetilde{\mathbb{Z}}^g_{\Gamma,\Lambda}\right) \propto \prod_{t=1}^{\Gamma-1}\left(\gamma_t^g\right)^{(b)}_{[i']}\prod_{n=1}^{\Lambda}\left(\tilde{\gamma}^g_{\Gamma,n}\right)^{(b)}_{[i]} P\left(x^g_\Gamma(n)=\mathcal{X}_i\middle|\left(\mathbb{x}^g_{\Gamma,n-1}\right)^{(b)}\right) \tag{36}$$

where $b=1,\ldots,\widetilde{B}_{\Gamma,\Lambda}$, $\{(\widetilde{\mathbb{X}}^g_{\Gamma,\Lambda})^{(b)}\}_{b=1}^{\widetilde{B}_{\Gamma,\Lambda}}$ contains all legal realizations of $\widetilde{\mathbb{X}}^g_{\Gamma,\Lambda}$, and $(\gamma_t^g)^{(b)}_{[i']}$ and $(\tilde{\gamma}^g_{\Gamma,n})^{(b)}_{[i]}$ are given in (19) and (31), respectively. Then we retain the β particles $\{(\widetilde{\mathbb{X}}^g_{\Gamma,\Lambda})^{(b)}\}_{b=1}^{\beta}$ with the highest *a posteriori* probabilities as the initial importance weights $\{(\varpi^g_{\Gamma,\Lambda})^{(b)}\}_{b=1}^{\beta}$, where $\beta \le \widetilde{B}_{\Gamma,\Lambda}$.

After the initialization, we update the importance weight according to (29). At each sampling interval on the basis of subcarrier, current β particles with the highest importance weights are selected as the survivors over $\beta|\tilde{\mathcal{X}}| = \beta(M+1)$ possible hypotheses departed from the previous particles. Specially, when the recursion reaches the last subcarrier of each subblock, i.e., $n=N$, the legality of the possible samples will be first examined according to (35) and β legal particles with the highest importance weights are selected as the survivors over those legal hypotheses. When the recursion reaches the bottom, i.e., $t=N_t$ and $n=N$, the particles associated with the importance weights are then used to compute the *a posteriori* probability for each subcarrier symbol in (26), given by

$$P\left(x_t^g(n)=\mathcal{X}_i\middle|\{\mathbf{z}_t^g\}_{t=1}^{N_t}\right) \cong \frac{1}{\widetilde{\varpi}^g_{N_t,N}}\sum_{b=1}^{\beta}\mathbb{I}\left(\left(x_t^g(n)\right)^{(b)};\mathcal{X}_i\right)\left(\varpi^g_{N_t,N}\right)^{(b)} \tag{37}$$

where $\mathcal{X}_i \in \tilde{\mathcal{X}}$ and $\widetilde{\varpi}^g_{N_t,N} = \sum_{b=1}^{\beta}(\varpi^g_{N_t,N})^{(b)}$. However, as emphasized above, due to the dependence of subcarriers within each subblock, we cannot estimate each symbol independently based on (37) as the demapping of OFDM-IM subblock may fail. Simply, by considering the joint estimation for active subcarriers and modulated symbols within each subblock, we can estimate the *a posteriori* probability for each subblock similar to (22) to solve this problem as follows:

$$P\left(\mathbf{x}_t^g=\mathbf{\Phi}_i\middle|\{\mathbf{z}_t^g\}_{t=1}^{N_t}\right) \cong \frac{1}{\widetilde{\varpi}^g_{N_t,N}}\sum_{b=1}^{\beta}\mathbb{I}\left(\left(\mathbb{x}^g_{t,N}\right)^{(b)};\mathbf{\Phi}_i\right)\left(\varpi^g_{N_t,N}\right)^{(b)} \tag{38}$$

where $(\mathbb{x}^g_{t,N})^{(b)}$ with $t=1,\ldots,N_t$ are extracted from $(\widetilde{\mathbb{X}}^g_{N_t,N})^{(b)}$ and $\mathbf{\Phi}_i \in \tilde{\mathbf{\Phi}}$. Finally, we summarize the deterministic SMC aided subcarrier-wise detection in Algorithm 2.

V. Complexity Analysis and Comparison

In this section, the computational complexity of the proposed SMC-based detectors is compared with the detectors developed in [40] and [41], where the detection complexity is measured by average NCM performed per subcarrier. To facilitate comparison, the number of receive antennas is assumed to be equal to the number of transmit antennas, i.e., $N_r = N_t$.

[5] If $\Gamma \ge N_t$ and $\Lambda \ge N$, we can compute $P(\widetilde{\mathbb{X}}^g_{N_t,N}|\widetilde{\mathbb{Z}}^g_{N_t,N})$ exactly based on the deterministic SMC; however, it is too computationally expensive.

Algorithm 2: Deterministic SMC Aided Subcarrier-wise Detection.

1: Perform the lower triangular operation to obtain (10);
2: Enumerate all legal realizations of $\widetilde{\mathbb{X}}^g_{\Gamma,\Lambda}$ with their *a posteriori* probabilities given in (36), and retain the β initial particles $\{(\widetilde{\mathbb{X}}^g_{\Gamma,\Lambda})^{(b)}\}_{b=1}^{\beta}$ with the highest *a posteriori* probabilities as the initial importance weights $\{(\varpi^g_{\Gamma,\Lambda})^{(b)}\}_{b=1}^{\beta}$;
3: **for** $n = \Lambda + 1$ to N **do**
4: Update and examine the particles associated with the importance weights according to (29) and (35), $b = 1, \ldots, \beta$;
5: **end for**
6: **for** $t = \Gamma + 1$ to N_t **do**
7: **for** $n = 1$ to N **do**
8: Update the importance weights according to (29), $b = 1, \ldots, \beta$;
9: **if** $n = N$ **then**
10: Compute ζ mapping for the K active subcarrier indices extracted from each hypothesis $\{(\mathbb{x}^g_{t,N-1})^{(b)}, \mathcal{X}_i\}$ according to (35), and set the importance weights for those illegal hypotheses ($\zeta \geq N_C$) to zeros, $b = 1, \ldots, \beta$, $i = 1, \ldots, M + 1$;
11: **end if**
12: Pick up and retain β particles with the highest importance weights among the $\beta|\tilde{\mathcal{X}}| = \beta(M + 1)$ hypotheses with the set of weights $\{(\varpi^g_{t,n})^{(b)}_{[i]}\}$, $b = 1, \ldots, \beta$, $i = 1, \ldots, M + 1$;
13: **end for**
14: **end for**
15: Compute the *a posteriori* probability for each subblock via (38), and the estimate of each subblock is given by $\widehat{\mathbf{x}}^g_t = \arg\max_{\mathbf{\Phi}_i \in \tilde{\mathbf{\Phi}}} P(\mathbf{x}^g_t = \mathbf{\Phi}_i \Big| \{\mathbf{z}^g_t\}_{t=1}^{N_t})$, $t = 1, \ldots, N_t$.

A. Complexity of Detectors in [40] and [41]

Explicitly, the complexity of the ML detector in (8) is given by

$$\mathcal{C}_{\text{ML}} = N_t \left(N_t + 1\right) \left(N_C M^K\right)^{N_t}. \tag{39}$$

After employing the MMSE filtering to eliminate the interference between the subblocks of different transmit antennas, the simple MMSE detector developed in [41] decodes the MIMO-OFDM-IM signal in a subblock-wise manner, whose complexity is

$$\mathcal{C}_{\text{simple MMSE}} = 7N_t^3 + N_t^2 + N_C M^K. \tag{40}$$

For the MMSE-LLR detection, the complexity is given by [40], [41]

$$\mathcal{C}_{\text{MMSE-LLR}} = 7N_t^3 + N_t \left(N_t + M + 1\right) \tag{41}$$

where a decomposition detection based on LLR calculation for each subcarrier is achieved after the MMSE filtering. Moreover, a novel OSIC based sequential MMSE-LLR detector, which referred to as MMSE-LLR-OSIC, is also proposed in [41] to further improve the error performance, whose complexity can be approximated as

$$\mathcal{C}_{\text{MMSE-LLR-OSIC}} \cong 3N_t^4 + 7N_t^3 + N_t \left(6N_t + M + 1\right). \tag{42}$$

B. Complexity of Proposed Detectors

As shown in Algorithms 1 and 2, the complexity of the proposed SMC-based detectors mainly consists of three parts:

- the lower triangular operation to construct the sequential structure for MIMO-OFDM-IM;
- the initialization of the importance weights;
- the update of the importance weights.

By using Householder transformations [52] to the QL decomposition, the complexity to construct the sequential structure of (10) for per subblock is given by

$$\mathcal{C}_{\text{QR}} \approx 2NN_t^3/3 + 2NN_t^2. \tag{43}$$

1) Proposed Subblock-wise Detection: For per subblock, the complexity of the initialization for the importance weights based on (21) is

$$\mathcal{C}_{\text{ini1}} = \beta N \cdot \Gamma \left(\Gamma + 5\right)/2 + \beta\Gamma \tag{44}$$

and the complexity of the update for the importance weights based on (18) from $(\Gamma + 1)$-th subblock to the last one is

$$\mathcal{C}_{\text{udp1}} = \beta N \cdot N_C M^K \cdot \left(N_t + \Gamma + 7\right)\left(N_t - \Gamma\right)/2. \tag{45}$$

After neglecting some lower order terms, the complexity in terms of average NCM performed per subcarrier for the proposed subblock-wise detection is given by

$$\begin{aligned}\mathcal{C}_{\text{pro1}} &= \left(\mathcal{C}_{\text{QR}} + \mathcal{C}_{\text{ini1}} + \mathcal{C}_{\text{upd1}}\right)/N \\ &\approx 2N_t^3/3 + 2N_t^2 + \left(N_t^2 - \Gamma^2\right)\beta N_C M^K/2.\end{aligned} \tag{46}$$

2) Proposed Subcarrier-wise Detection: For per subblock, the complexity of the initialization for the importance weights in (36) is

$$\begin{aligned}\mathcal{C}_{\text{ini2}} &= \beta N \cdot \left(\Gamma - 1\right)\left(\Gamma + 4\right)/2 \\ &\quad + \beta\Lambda \cdot \left(\Gamma + 2\right) + \beta\left(\Gamma - 1 + 2\Lambda\right)\end{aligned} \tag{47}$$

and the complexity of the update for the importance weights based on (29) to the rest of the subcarriers is

$$\begin{aligned}\mathcal{C}_{\text{udp2}} &= \beta N \cdot \left(M + 1\right) \cdot \left(N_t + \Gamma + 9\right)\left(N_t - \Gamma\right)/2 \\ &\quad + \beta\left(N - \Lambda\right) \cdot \left(M + 1\right)\left(N_t + 4\right).\end{aligned} \tag{48}$$

Therefore, the complexity in terms of average NCM performed per subcarrier for the proposed subcarrier-wise detection is given by

$$\begin{aligned}\mathcal{C}_{\text{pro2}} &= \left(\mathcal{C}_{\text{QR}} + \mathcal{C}_{\text{ini2}} + \mathcal{C}_{\text{upd2}}\right)/N \\ &\approx 2N_t^3/3 + 2N_t^2 + \left(N_t^2 - \Gamma^2\right)\beta(M + 1)/2\end{aligned} \tag{49}$$

where the lower order terms have been neglected in (49). However, to be more accurate, exact NCM without neglecting any terms will be compared for different types of detectors in the numerical results of Section VI.

In Table I, a brief summary of the computational complexity measured by the average NCM for different detectors of MIMO-OFDM-IM is provided. As seen from Table I, the brute-force

TABLE I
DECODING COMPLEXITY COMPARISONS IN TERMS OF AVERAGE NCM PERFORMED PER SUBCARRIER

Detector	Computational complexity	Order of complexity
Brute-Force ML	$N_t\left(N_t+1\right)\left(N_C M^K\right)^{N_t}$	$\mathcal{O}\left(M^{KN_t}\right)$
Simple MMSE	$7N_t^3+N_t^2+N_C M^K$	$\mathcal{O}\left(M^K\right)$
MMSE-LLR	$7N_t^3+N_t\left(N_t+M+1\right)$	$\mathcal{O}\left(M\right)$
MMSE-LLR-OSIC	$\cong 3N_t^4+7N_t^3+N_t\left(6N_t+M+1\right)$	$\mathcal{O}\left(M\right)$
Proposed subblock-wise detection	$2N_t^3/3+2N_t^2+\left(N_t^2-\Gamma^2\right)\beta N_C M^K/2$	$\mathcal{O}\left(M^K\right)$
Proposed subcarrier-wise detection	$2N_t^3/3+2N_t^2+\left(N_t^2-\Gamma^2\right)\beta(M+1)/2$	$\mathcal{O}\left(M\right)$

ML detection leads to prohibitive computational complexity and the highest order of detection complexity with respect to the constellation size M. The proposed subblock-wise detection requires much lower computational complexity than the brute-force ML detection while the proposed subcarrier-wise detection shows the same level of computational complexity as the MMSE-LLR method.

VI. SIMULATION AND NUMERICAL RESULTS

In this section, we verify the effectiveness of the proposed detection algorithms for MIMO-OFDM-IM via computer simulation and numerical results. In the computer simulations, a MIMO channel with frequency-selective Rayleigh fading is considered, where the maximum delay spread of the channel is equal to $10\times T_s$, where T_s denotes the sampling period of the digital system. Each OFDM-IM block consists of $N_F=512$ subcarriers and is appended by a CP of length $N_{cp}=16$. It is assumed that channel state information is unknown to the transmitter but perfectly known to the receiver. For ease of comparison, the number of receive antennas is set to be equal to the number of transmit antennas, i.e., $N_r=N_t$. To initialize the SMC process, we set $\Gamma=1$ for Algorithm 1, and $\Gamma=1$ and $\Lambda=N$ for Algorithm 2. Moreover, for fair comparison, we adopt the same number of particles β for both deterministic SMC aided detection methods in the following simulations.

A. Error Performance Comparison

Fig. 5 shows the BER comparison results of different detection algorithms for the MIMO-OFDM-IM system with $N_t=4$, $K=1$, and QPSK modulation. As seen from Fig. 5, the proposed subblock-wise detector achieves near-optimal BER performance for the MIMO-OFDM-IM system with reduced complexity for both $N=2$ and $N=4$ cases. Although the proposed subcarrier-wise detector is slightly inferior to the subblock-wise detector, it is favorable for its lower computational complexity than that of the subblock-wise one, which will be shown in the next subsection. Both our detectors show considerably better performance than those of MMSE based detectors. Specially, the simple MMSE and MMSE-LLR detectors suffer from a significant performance loss and their diversity order is always equal to one. On the other hand, both proposed detectors show to attain the same diversity order as the ML detection.

Fig. 6 shows the BER comparison results of different detection algorithms for the MIMO-OFDM-IM system with $N_t=4$, $N=4$, and BPSK modulation. It can be observed that similarly the proposed subblock-wise detector achieves near-optimal performance while the proposed subcarrier-wise detector only suffers from a marginal performance loss compared to the ML detection. Although the MMSE-LLR-OSIC detector outperforms the other two MMSE based detectors at the cost of a higher complexity, its performance is still far from optimal (ML detection). By comparing the two scenarios with different number of active subcarriers ($K=1$ and $K=2$), we observe that the BER performance of all detectors degrades as the number of active subcarriers increases. This can be understood as each active subcarrier will be allocated less power when more subcarriers are activated simultaneously for transmission.

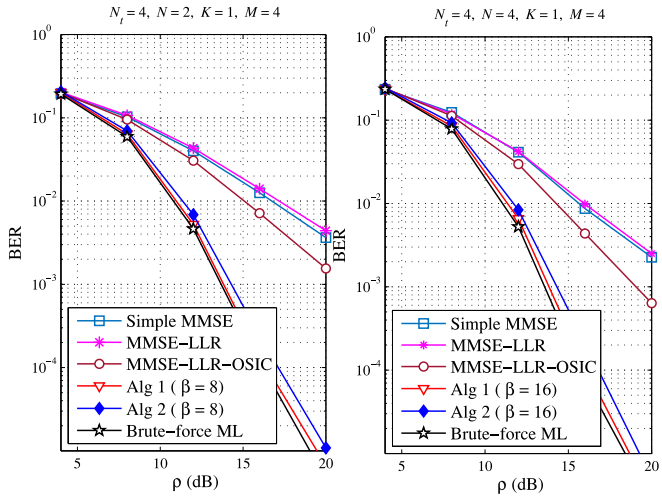

Fig. 5. BER performance comparison of different detection algorithms for MIMO-OFDM-IM with $N_t=4$, $K=1$, and QPSK modulation.

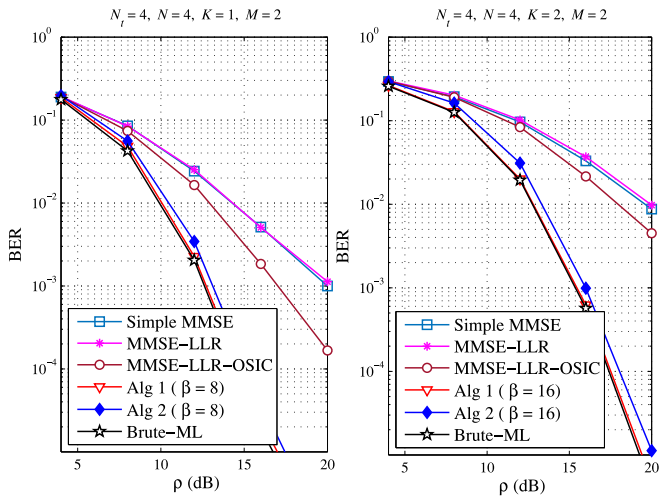

Fig. 6. BER performance comparison of different detection algorithms for MIMO-OFDM-IM with $N_t=4$, $N=4$, and BPSK modulation.

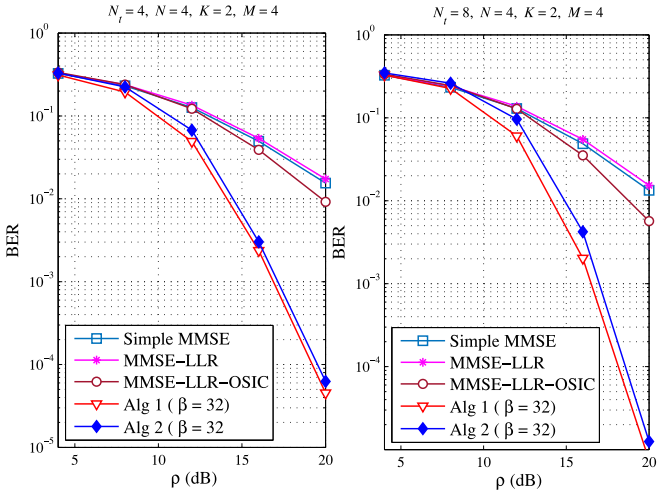

Fig. 7. BER performance comparison of different detection algorithms for MIMO-OFDM-IM with $N = 4$, $K = 2$, and QPSK modulation.

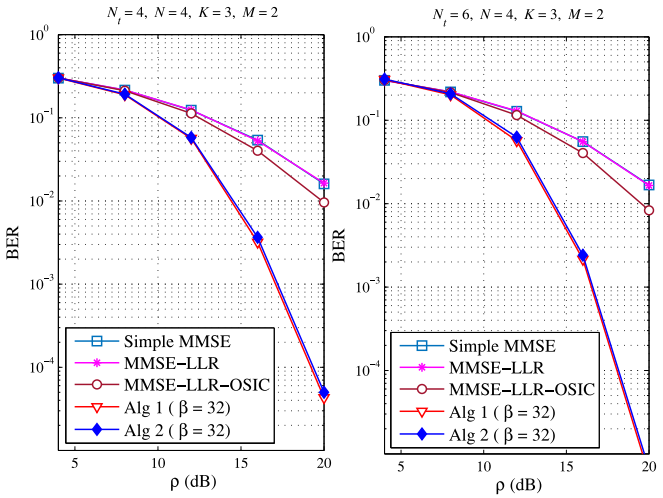

Fig. 8. BER performance comparison of different detection algorithms for MIMO-OFDM-IM with $N = 4$, $K = 3$, and BPSK modulation.

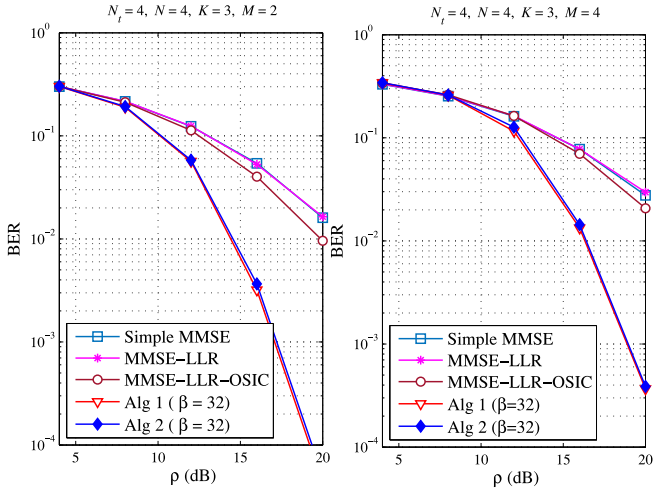

Fig. 9. BER performance comparison of different detection algorithms for MIMO-OFDM-IM with $N_t = 4$, $N = 4$, and $K = 3$.

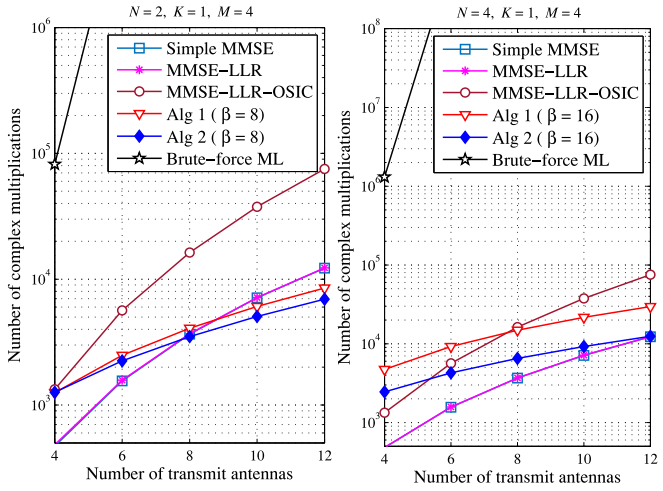

Fig. 10. Complexity comparison of different detection algorithms for MIMO-OFDM-IM with $K = 1$, and QPSK modulation.

In Fig. 7, the BER performance of different detection algorithms is compared for the MIMO-OFDM-IM system with $N = 4$, $K = 2$, and QPSK modulation. As the ML detection requires an immense amount of computation, its BER curve is not shown in Fig. 7. It can be seen that the proposed detectors outperform the MMSE based detectors significantly. Moreover, we observe that unlike the simple MMSE and MMSE-LLR detectors, the BER performance of both proposed detectors is improved as the number of receive antennas ($N_r = N_t$) increases. This can be understood since the diversity order of the simple MMSE and MMSE-LLR detectors is equal to one regardless of the number of receive antennas while a diversity order of N_r is obtained by both proposed detectors.

In Fig. 8, the BER performance of different detection algorithms is compared for the MIMO-OFDM-IM system with $N = 4$, $K = 4$, and BPSK modulation. From Fig. 8, we observe that the subcarrier-wise detector also has the potential to achieve almost the same performance as the subblock-wise one for this configuration. This can be understood since both proposed detectors can approach the optimal performance when the number of particles is large enough (e.g., $\beta = 32$). Therefore, the deterministic SMC aided detectors are able to provide a flexible trade-off between the computational complexity and the error performance by adjusting the number of particles.

Fig. 9 shows the BER comparison results of different detection algorithms for the MIMO-OFDM-IM system with $N_t = 4$, $N = 4$, and $K = 3$. It still can be observed that when the number of particles is large enough, the subcarrier-wise detector achieves almost the same performance as the subblock-wise one for different modulation orders. Moreover, the performance of all detectors degrades with the increase of the modulation orders. Specially, the performance gain of the MMSE-LLR-OSIC detector over the MMSE-LLR one is smaller with higher modulation orders.

B. Complexity Comparison

In Figs. 10 and 11, the computational complexity for different types of detectors is compared in terms of exact NCM performed per subcarrier. As expected, the computational complexity of the ML detection is prohibitive and increases exponentially with the

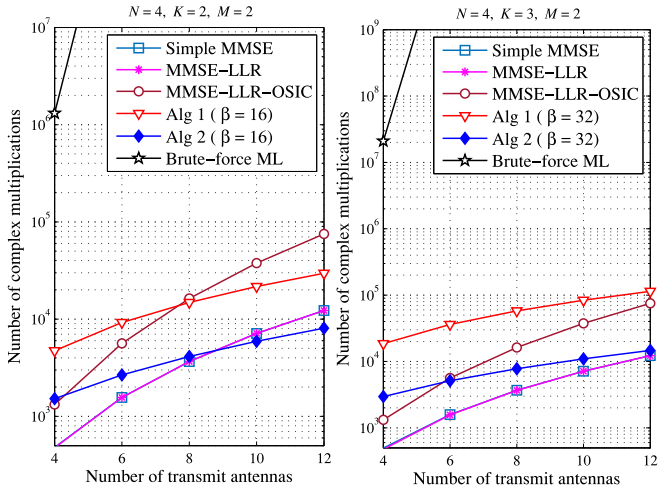

Fig. 11. Complexity comparison of different detection algorithms for MIMO-OFDM-IM with $N = 4$, and BPSK modulation.

number of transmit antennas. However, our proposed detectors achieve rather low computational complexity, which is comparable to that of MMSE based detectors. Interestingly, the computational complexity of the MMSE-LLR-OSIC detector seems to be more susceptible to the number of transmit antennas and the subcarrier-wise detector has the potential to achieve a lower complexity than the MMSE-LLR detector when the number of transmit antennas increases. On the other hand, the computational complexity of the subblock-wise detector is sensitive to the size of subblock and is always higher than that of the subcarrier-wise one.

In summary, the proposed detection algorithms are able to provide an effective trade-off between BER performance and computational complexity. Moreover, the proposed detection algorithms achieve near-optimal performance while maintaining considerably lower complexity that is comparable to that of the simple MMSE and MMSE-LLR detectors.

VII. Conclusion

In this paper, we have proposed two low-complexity detectors derived from the SMC theory for the MIMO-OFDM-IM system. The first proposed subblock-wise detector draws samples at the subblock level, exhibiting near-optimal performance for the MIMO-OFDM-IM system. The second proposed subcarrier-wise detector draws samples at the subcarrier level, exhibiting substantially reduced complexity with a marginal performance loss. An effective legality examination method has been also developed to couple with the subcarrier-wise detector. Computer simulation and numerical results have validated the outstanding performance and the low complexity of both proposed detectors.

Appendix A
Proof of Proposition 1

According to [50] and [43], the importance weight is given by

$$\left(\varpi_t^g\right)^{(b)} = \frac{P\left(\left(\mathbb{X}_t^g\right)^{(b)} \middle| \mathbb{Z}_t^g\right)}{\psi\left(\left(\mathbb{X}_t^g\right)^{(b)} \middle| \mathbb{Z}_t^g\right)}. \tag{50}$$

Although (50) is not sequential, we can come up with a sequential version by exploiting the property of the trial distribution. In order to work in a sequential manner, the trial distribution is supposed to satisfy

$$\psi\left(\mathbb{X}_t^g \middle| \mathbb{Z}_t^g\right) = \psi\left(\mathbb{X}_1^g \middle| \mathbb{Z}_1^g\right) \prod_{t'=2}^{t} \psi\left(\mathbf{x}_{t'}^g \middle| \mathbb{X}_{t'-1}^g, \mathbb{Z}_{t'}^g\right). \tag{51}$$

Furthermore, (51) can be rewritten in a recursive form as

$$\psi\left(\mathbb{X}_t^g \middle| \mathbb{Z}_t^g\right) = \psi\left(\mathbb{X}_{t-1}^g \middle| \mathbb{Z}_{t-1}^g\right) \psi\left(\mathbf{x}_t^g \middle| \mathbb{X}_{t-1}^g, \mathbb{Z}_t^g\right). \tag{52}$$

Based on (50) and (52), the update recursions for the importance weights are then given by

$$\left(\varpi_t^g\right)^{(b)} = \left(\varpi_{t-1}^g\right)^{(b)} \times \frac{P\left(\left(\mathbb{X}_t^g\right)^{(b)} \middle| \mathbb{Z}_t^g\right)}{\psi\left(\left(\mathbb{X}_{t-1}^g\right)^{(b)} \middle| \mathbb{Z}_{t-1}^g\right) \psi\left(\left(\mathbf{x}_t^g\right)^{(b)} \middle| \left(\mathbb{X}_{t-1}^g\right)^{(b)}, \mathbb{Z}_t^g\right)} \tag{53}$$

where $b = 1, \ldots, \beta$. With the trial distribution of (14) satisfying (52), (53) can be further written as

$$\left(\varpi_t^g\right)^{(b)} \propto \left(\varpi_{t-1}^g\right)^{(b)} \times \frac{P\left(\left(\mathbb{X}_t^g\right)^{(b)} \middle| \mathbb{Z}_t^g\right)}{P\left(\left(\mathbb{X}_{t-1}^g\right)^{(b)} \middle| \mathbb{Z}_{t-1}^g\right) P\left(\left(\mathbf{x}_t^g\right)^{(b)} \middle| \left(\mathbb{X}_{t-1}^g\right)^{(b)}, \mathbb{Z}_t^g\right)} \tag{54}$$

$$= \left(\varpi_{t-1}^g\right)^{(b)} \cdot \frac{P\left(\left(\mathbb{X}_{t-1}^g\right)^{(b)} \middle| \mathbb{Z}_t^g\right)}{P\left(\left(\mathbb{X}_{t-1}^g\right)^{(b)} \middle| \mathbb{Z}_{t-1}^g\right)} \tag{55}$$

$$\propto \left(\varpi_{t-1}^g\right)^{(b)} \cdot p\left(\mathbf{z}_t^g \middle| \mathbb{Z}_{t-1}^g, \left(\mathbb{X}_{t-1}^g\right)^{(b)}\right) \tag{56}$$

$$= \left(\varpi_{t-1}^g\right)^{(b)} \cdot p\left(\mathbf{z}_t^g \middle| \left(\mathbb{X}_{t-1}^g\right)^{(b)}\right) \tag{57}$$

where (55) holds due to the independence of the previous particle $\left(\mathbb{X}_{t-1}^g\right)^{(b)}$ and the current subblock $\mathbf{x}_t^g$, (56) is obtained by neglecting the constant term $p\left(\mathbb{Z}_{t-1}^g\right)/p\left(\mathbb{Z}_t^g\right)$, and (57) holds due to the independence of the noise samples, completing the proof.

Appendix B
Proof of Proposition 2

Similar to the proof of *Proposition 1*, the update recursions for importance weights are given by

$$\left(\varpi_{t,n}^g\right)^{(b)} = \left(\varpi_{t,n-1}^g\right)^{(b)} \times \frac{P\left(\left(\widetilde{\mathbb{X}}_{t,n}^g\right)^{(b)} \middle| \widetilde{\mathbb{Z}}_{t,n}^g\right)}{\psi\left(\left(\widetilde{\mathbb{X}}_{t,n-1}^g\right)^{(b)} \middle| \widetilde{\mathbb{Z}}_{t,n-1}^g\right) \psi\left(\left(\widetilde{\mathbb{X}}_{t,n}^g\right)^{(b)} \middle| \left(\widetilde{\mathbb{X}}_{t,n-1}^g\right)^{(b)}, \widetilde{\mathbb{Z}}_{t,n}^g\right)} \tag{58}$$

where $b = 1, \ldots, \beta$. With the trial distribution of (27), (58) can be further written as

$$\left(\varpi_{t,n}^{g}\right)^{(b)} \propto \left(\varpi_{t,n-1}^{g}\right)^{(b)} \times \frac{P\left(\left(\widetilde{\mathbb{X}}_{t,n}^{g}\right)^{(b)} \middle| \widetilde{\mathbb{Z}}_{t,n}^{g}\right)}{P\left(\left(\widetilde{\mathbb{X}}_{t,n-1}^{g}\right)^{(b)} \middle| \widetilde{\mathbb{Z}}_{t,n-1}^{g}\right) P\left(\left(\widetilde{\mathbb{X}}_{t,n}^{g}\right)^{(b)} \middle| \left(\widetilde{\mathbb{X}}_{t,n-1}^{g}\right)^{(b)}, \widetilde{\mathbb{Z}}_{t,n}^{g}\right)}$$

$$= \left(\varpi_{t,n-1}^{g}\right)^{(b)} \cdot \frac{P\left(\left(\widetilde{\mathbb{X}}_{t,n-1}^{g}\right)^{(b)} \middle| \widetilde{\mathbb{Z}}_{t,n}^{g}\right)}{P\left(\left(\widetilde{\mathbb{X}}_{t,n-1}^{g}\right)^{(b)} \middle| \widetilde{\mathbb{Z}}_{t,n-1}^{g}\right)} \tag{59}$$

$$\propto \left(\varpi_{t,n-1}^{g}\right)^{(b)} \cdot p\left(z_t^g(n) \middle| \widetilde{\mathbb{Z}}_{t,n-1}^{g}, \left(\widetilde{\mathbb{X}}_{t,n-1}^{g}\right)^{(b)}\right) \tag{60}$$

$$= \left(\varpi_{t,n-1}^{g}\right)^{(b)} \cdot p\left(z_t^g(n) \middle| \left(\widetilde{\mathbb{X}}_{t,n-1}^{g}\right)^{(b)}\right) \tag{61}$$

where (60) is obtained by neglecting the constant term $p(\widetilde{\mathbb{Z}}_{t,n-1}^{g})/p(\widetilde{\mathbb{Z}}_{t,n}^{g})$, and (61) holds due to the independence of the noise samples, completing the proof.

REFERENCES

[1] E. G. Larsson, O. Edfors, F. Tufvesson, and T. L. Marzetta, "Massive MIMO for next generation wireless systems," *IEEE Commun. Mag.*, vol. 52, no. 2, pp. 186–195, Feb. 2014.

[2] S. Sun, T. S. Rappaport, R. W. Heath, A. Nix, and S. Rangan, "MIMO for millimeter-wave wireless communications: Beamforming, spatial multiplexing, or both?" *IEEE Commun. Mag.*, vol. 52, no. 12, pp. 110–121, Dec. 2014.

[3] D. Tse and P. Viswanath, *Fundamentals of Wireless Communication*. Cambridge, UK: Cambridge Univ. Press, 2005.

[4] R. Y. Mesleh, H. Haas, S. Sinanovic, C. W. Ahn, and S. Yun, "Spatial modulation," *IEEE Trans. Veh. Technol.*, vol. 57, no. 4, pp. 2228–2241, Jul. 2008.

[5] M. D. Renzo, H. Haas, and P. M. Grant, "Spatial modulation for multiple-antenna wireless systems: A survey," *IEEE Commun. Mag.*, vol. 49, no. 12, pp. 182–191, Dec. 2011.

[6] M. D. Renzo, H. Haas, A. Ghrayeb, S. Sugiura, and L. Hanzo, "Spatial modulation for generalized MIMO: Challenges, opportunities, and implementation," *Proc. IEEE*, vol. 102, no. 1, pp. 56–103, Jan. 2014.

[7] P. Yang, M. D. Renzo, Y. Xiao, S. Li, and L. Hanzo, "Design guidelines for spatial modulation," *IEEE Commun. Surveys Tuts.*, vol. 17, no. 1, pp. 6–26, Jan.–Mar. 2015.

[8] E. Basar, "Index modulation techniques for 5G wireless networks," *IEEE Commun. Mag.*, vol. 54, no. 7, pp. 168–175, Jul. 2016.

[9] P. Yang, Y. Xiao, B. Zhang, S. Li, M. El-Hajjar, and L. Hanzo, "Power allocation-aided spatial modulation for limited-feedback MIMO systems," *IEEE Trans. Veh. Technol.*, vol. 64, no. 5, pp. 2198–2204, May 2015.

[10] P. Yang, Y. L. Guan, Y. Xiao, M. D. Renzo, S. Li, and L. Hanzo, "Transmit precoded spatial modulation: Maximizing the minimum euclidean distance versus minimizing the bit error ratio," *IEEE Trans. Wireless Commun.*, vol. 15, no. 3, pp. 2054–2068, Mar. 2016.

[11] P. Yang, Y. Xiao, L. Li, Q. Tang, Y. Yu, and S. Li, "Link adaptation for spatial modulation with limited feedback," *IEEE Trans. Veh. Technol.*, vol. 61, no. 8, pp. 3808–3813, Oct. 2012.

[12] P. Yang, Y. Xiao, Y. Yu, and S. Li, "Adaptive spatial modulation for wireless MIMO transmission systems," *IEEE Commun. Lett.*, vol. 15, no. 6, pp. 602–604, Jun. 2011.

[13] P. Yang, Y. Xiao, Y. Yu, L. Li, Q. Tang, and S. Li, "Simplified adaptive spatial modulation for limited-feedback MIMO systems," *IEEE Trans. Veh. Technol.*, vol. 62, no. 6, pp. 2656–2666, Jul. 2013.

[14] Y. Xiao, Z. Yang, L. Dan, P. Yang, L. Yin, and W. Xiang, "Low-complexity signal detection for generalized spatial modulation," *IEEE Commun. Lett.*, vol. 18, no. 3, pp. 403–406, Mar. 2014.

[15] L. Xiao *et al.*, "Efficient compressed sensing detectors for generalized spatial modulation systems," *IEEE Trans. Veh. Technol.*, vol. 66, no. 2, pp. 1284–1298, Feb. 2017.

[16] L. Xiao *et al.*"An improved soft-input soft-output detector for generalized spatial modulation," *IEEE Signal Process. Lett.*, vol. 23, no. 1, pp. 30–34, Jan. 2016.

[17] A. Stavridis, S. Sinanovic, M. D. Renzo, and H. Haas, "Energy evaluation of spatial modulation at a multi-antenna base station," in *Proc. IEEE Veh. Technol. Conf.*, Las Vegas, USA, Sep. 2013, pp. 1–5.

[18] A. Stavridis, S. Sinanovic, M. D. Renzo, H. Haas, and P. Grant, "An energy saving base station employing spatial modulation," in *Proc. IEEE Comput. Aided Model. Design Commun. Links Netw.*, Barcelona, Spain, Sep. 2012, pp. 231–235.

[19] A. Stavridis, S. Sinanovic, M. D. Renzo, and H. Haas, "A power saving dual-hop architecture based on hybrid spatial modulation," in *Proc. IEEE Asilomar Conf. Signals, Syst. Comput.*, Pacific Grove, CA, USA, Nov. 2012, pp. 1366–1370.

[20] M. C. Lee and W. H. Chung, "Spectral efficiency and energy efficiency optimization via mode selection for spatial modulation in MIMO systems," *IEEE Trans. Veh. Technol.*, to be published.

[21] P. Yang *et al.*"Single-carrier SM-MIMO: A promising design for broadband large-scale antenna systems," *IEEE Commun. Surveys Tuts.*, vol. 18, no. 3, pp. 1687–1716, Jul.–Sep. 2016.

[22] L. Xiao, L. Dan, Y. Zhang, Y. Xiao, P. Yang, and S. Li, "A low-complexity detection scheme for generalized spatial modulation aided single carrier systems," *IEEE Commun. Lett.*, vol. 19, no. 6, pp. 1069–1072, Jun. 2015.

[23] L. Xiao, P. Yang, Y. Zhao, Y. Xiao, J. Liu, and S. Li, "Low-complexity tree search-based detection algorithms for generalized spatial modulation aided single carrier systems," in *Proc. IEEE Int. Conf. Commun.*, Kuala Lumpur, Malaysia, May 2016, pp. 1–6.

[24] R. Abu-alhiga and H. Haas, "Subcarrier-index modulation OFDM," in *Proc. IEEE Int. Symp. Personal, Indoor, Mobile Radio Commun.*, Tokyo, Japan, Sep. 2009, pp. 177–181.

[25] D. Tsonev, S. Sinanovic, and H. Haas, "Enhanced subcarrier index modulation (SIM) OFDM," in *Proc. IEEE Global Commun. Conf.*, Houston, USA, Dec. 2011, pp. 728–732.

[26] E. Basar, U. Aygolu, E. Panayirci, and H. V. Poor, "Orthogonal frequency division multiplexing with index modulation," *IEEE Trans. Signal Process.*, vol. 61, no. 22, pp. 5536–5549, Nov. 2013.

[27] M. Wen, X. Cheng, and L. Yang, *Index Modulation for 5G Wireless Communications* (Wireless Networks Series). Berlin, Germany: Springer, 2017.

[28] B. Zheng, F. Chen, M. Wen, F. Ji, H. Yu, and Y. Liu, "Low-complexity ML detector and performance analysis for OFDM with in-phase/quadrature index modulation," *IEEE Commun. Lett.*, vol. 19, no. 11, pp. 1893–1896, Nov. 2015.

[29] Y. Xiao, S. Wang, L. Dan, X. Lei, P. Yang, and W. Xiang, "OFDM with interleaved subcarrier-index modulation," *IEEE Commun. Lett.*, vol. 18, no. 8, pp. 1447–1450, Aug. 2014.

[30] X. Cheng, M. Wen, L. Yang, and Y. Li, "Index modulated OFDM with interleaved grouping for V2X communications," in *Proc. IEEE Int. Conf. Intell. Transport. Syst.*, Qingdao, China, Oct. 2014, pp. 1097–1104.

[31] E. Basar, "OFDM with index modulation using coordinate interleaving," *IEEE Wireless Commun. Lett.*, vol. 4, no. 4, pp. 381–384, Aug. 2015.

[32] R. Fan, Y. J. Yu, and Y. L. Guan, "Generalization of orthogonal frequency division multiplexing with index modulation," *IEEE Trans. Wireless Commun.*, vol. 14, no. 10, pp. 5350–5359, Oct. 2015.

[33] T. Datta, H. S. Eshwaraiah, and A. Chockalingam, "Generalized space-and-frequency index modulation," *IEEE Trans. Veh. Technol.*, vol. 65, no. 7, pp. 4911–4924, Jul. 2016.

[34] Y. Li, M. Zhang, X. Cheng, M. Wen, and L. Yang, "Index modulated OFDM with intercarrier interference cancellation," in *Proc. IEEE Int. Conf. Commun.*, Kuala Lumpur, Malaysia, May 2016, pp. 1–6.

[35] M. Wen, X. Cheng, L. Yang, Y. Li, X. Cheng, and F. Ji, "Index modulated OFDM for underwater acoustic communications," *IEEE Commun. Mag.*, vol. 54, no. 5, pp. 132–137, May 2016.

[36] M. Wen, X. Cheng, and L. Yang, "Optimizing the energy efficiency of OFDM with index modulation," in *Proc. IEEE Int. Conf. Commun. Syst.*, Macau, China, Nov. 2014, pp. 31–35.

[37] W. Li, H. Zhao, C. Zhang, L. Zhao, and R. Wang, "Generalized selecting sub-carrier modulation scheme in OFDM system," in *Proc. IEEE Int. Conf. Commun. Workshop*, Sydney, Australia, Jun. 2014, pp. 907–911.

[38] M. Wen, X. Cheng, M. Ma, B. Jiao, and H. V. Poor, "On the achievable rate of OFDM with index modulation," *IEEE Trans. Signal Process.*, vol. 64, no. 8, pp. 1919–1932, Apr. 2016.

[39] N. Ishikawa, S. Sugiura, and L. Hanzo, "Subcarrier-index modulation aided OFDM–Will it work?" *IEEE Access*, vol. 4, pp. 2580–2593, Jun. 2016.

[40] E. Basar, "Multiple-input multiple-output OFDM with index modulation," *IEEE Signal Process. Lett.*, vol. 22, no. 12, pp. 2259–2263, Dec. 2015.

[41] E. Basar, "On multiple-input multiple-output OFDM with index modulation for next generation wireless networks," *IEEE Trans. Signal Process.*, vol. 64, no. 15, pp. 3868–3878, Aug. 2016.

[42] E. Basar, E. Panayirci, M. Uysal, and H. Haas, "Generalized LED index modulation optical OFDM for MIMO visible light communications systems," in *Proc. IEEE Int. Conf. Commun.*, Kuala Lumpur, Malaysia, May 2016, pp. 1–5.
[43] B. Dong, X. Wang, and A. Doucet, "A new class of soft MIMO demodulation algorithms," *IEEE Trans. Signal Process.*, vol. 51, no. 11, pp. 2752–2763, Nov. 2003.
[44] C. J. Bordin and M. G. S. Bruno, "Sequential Bayesian algorithms for identification and blind equalization of unit-norm channels," *IEEE Signal Process. Lett.*, vol. 22, no. 11, pp. 2157–2161, Nov. 2015.
[45] P. Aggarwal, N. Prasad, and X. Wang, "An enhanced deterministic sequential Monte Carlo method for near-optimal MIMO demodulation with QAM constellations," *IEEE Trans. Signal Process.*, vol. 55, no. 6, pp. 2395–2406, Jun. 2007.
[46] P. Aggarwal and X. Wang, "Multilevel sequential Monte Carlo algorithms for MIMO demodulation," *IEEE Trans. Wireless Commun.*, vol. 6, no. 2, pp. 750–758, Feb. 2007.
[47] B. Li, C. Zhao, M. Sun, H. Zhang, Z. Zhou, and A. Nallanathan, "A Bayesian approach for nonlinear equalization and signal detection in millimeter-wave communications," *IEEE Trans. Wireless Commun.*, vol. 14, no. 7, pp. 3794–3809, Jul. 2015.
[48] Y. Yang, J. F. Hu, and H. L. Zhang, "Bit-level deterministic sequential Monte Carlo method for MIMO wireless systems," in *Proc. IEEE Int. Conf. Commun.*, Beijing, China, May 2008, pp. 3622–3626.
[49] J.-K. Zhang, A. Kavcic, and K. M. Wong, "Equal-diagonal QR decomposition and its application to precoder design for successive-cancellation detection," *IEEE Trans. Inf. Theory*, vol. 51, no. 1, pp. 154–172, Jan. 2005.
[50] A. Doucet, S. Godsill, and C. Andrieu, "On sequential Monte Carlo sampling methods for Bayesian filtering," *Statistics Comput.*, vol. 10, no. 3, pp. 197–208, 2000.
[51] R. Chen, X. Wang, and J. S. Liu, "Adaptive joint detection and decoding in flat-fading channels via mixture Kalman filtering," *IEEE Trans. Inf. Theory*, vol. 46, no. 6, pp. 2079–2094, Sep. 2000.
[52] N. J. Higham, *Accuracy and Stability of Numerical Algorithms*. Philadelphia, PA, USA: SIAM, 2002.

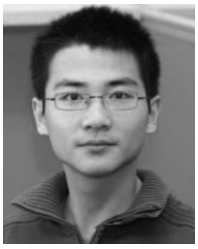

Beixiong Zheng received the B.S. degree from South China University of Technology, Guangzhou, China, in 2013, where he is currently working toward the Ph.D. degree.

Since December 2015, he has been a Visiting Student Research Collaborator with Columbia University, New York, NY, USA. His recent research interests include spatial modulation, nonorthogonal multiple access, and pilot multiplexing techniques. He received the Best Paper Award from the IEEE International Conference on Computing, Networking and Communications in 2016.

Miaowen Wen (M'14) received the B.S. degree from Beijing Jiaotong University, Beijing, China, in 2009, and the Ph.D. degree from Peking University, Beijing, China, in 2014. From 2012 to 2013, he was a Visiting Student Research Collaborator with Princeton University, Princeton, NJ, USA. Since 2014, he has been a Faculty Member with South China University of Technology, Guangzhou, China. He has authored a book and more than 50 papers in refereed journals and conference proceedings. His research interests include index modulation and non-orthogonal multiple access techniques.

Dr. Wen received the Best Paper Award from the IEEE International Conference on Intelligent Transportation Systems Telecommunications in 2012, the IEEE International Conference on Intelligent Transportation Systems in 2014, and the IEEE International Conference on Computing, Networking and Communications in 2016. He received the Excellent Doctoral Dissertation Award from Peking University. He is serving as a Guest Editor for a Special Section at IEEE ACCESS.

Ertugrul Basar (S'09–M'13–SM'16) received the B.S. degree with high honors from Istanbul University, Istanbul, Turkey, in 2007, and the M.S. and Ph.D. degrees from Istanbul Technical University, Istanbul, Turkey, in 2009 and 2013, respectively. He spent the academic year 2011–2012 in the Department of Electrical Engineering, Princeton University, Princeton, NJ, USA. He is currently an Assistant Professor in the Department of Electronics and Communication Engineering, Istanbul Technical University, and a Member of the Wireless Communication Research Group. His primary research interests include MIMO systems, index modulation, cooperative communications, OFDM, and visible light communications. He received the Istanbul Technical University Best Ph.D. Thesis Award in 2014 and three Best Paper Awards including one from IEEE International Conference on Communications. He currently serves as an Associate Editor for IEEE COMMUNICATIONS LETTERS and IEEE ACCESS. He is also a regular Reviewer for various IEEE journals, and has served as the TPC Member for several conferences. He is an Inventor of two pending patents on index modulation schemes.

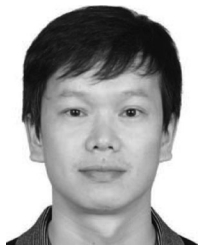

Fangjiong Chen (M'06) received the B.S. degree in electronics and information technology from Zhejiang University, Hangzhou China, in 1997, and the Ph.D. degree in communication and information engineering from South China University of Technology, Guangzhou, China, in 2002. After graduation, he joined the School of Electronics and Information Engineering, South China University of Technology. From 2002 to 2005, he was a Lecture and an Associate Professor from 2005 to 2011.

He is currently a full-time Professor in the School of Electronics and Information Engineering, South China University of Technology. He is also the Director of the Department of Underwater Detection and Imaging, Mobile Ultrasonic Detection National Research Center of Engineering Technology. His research focuses on signal detection and estimation, array signal processing, and wireless communication.

Dr. Chen received the National Science Fund for Outstanding Young Scientists in 2013, and was elected in the New Century Excellent Talent Program of MOE, China, in 2012.